

*ARMY RESEARCH LABORATORY*



**Geometric Single-Qubit Quantum Gates for an Electron Spin in  
a Quantum Dot**

**by Vladimir S. Malinovsky and Sergey Rudin**

**ARL-TR-6641**

**September 2013**

## **NOTICES**

### **Disclaimers**

The findings in this report are not to be construed as an official Department of the Army position unless so designated by other authorized documents.

Citation of manufacturer's or trade names does not constitute an official endorsement or approval of the use thereof.

Destroy this report when it is no longer needed. Do not return it to the originator.

# Army Research Laboratory

Adelphi, MD 20783-1197

---

ARL-TR-6641

September 2013

---

## Geometric Single-Qubit Quantum Gates for an Electron Spin in a Quantum Dot

Vladimir S. Malinovsky and Sergey Rudin

Sensors and Electron Devices Directorate, ARL

REPORT DOCUMENTATION PAGE			Form Approved OMB No. 0704-0188		
Public reporting burden for this collection of information is estimated to average 1 hour per response, including the time for reviewing instructions, searching existing data sources, gathering and maintaining the data needed, and completing and reviewing the collection information. Send comments regarding this burden estimate or any other aspect of this collection of information, including suggestions for reducing the burden, to Department of Defense, Washington Headquarters Services, Directorate for Information Operations and Reports (0704-0188), 1215 Jefferson Davis Highway, Suite 1204, Arlington, VA 22202-4302. Respondents should be aware that notwithstanding any other provision of law, no person shall be subject to any penalty for failing to comply with a collection of information if it does not display a currently valid OMB control number. <b>PLEASE DO NOT RETURN YOUR FORM TO THE ABOVE ADDRESS.</b>					
1. REPORT DATE (DD-MM-YYYY) September 2013		2. REPORT TYPE Final		3. DATES COVERED (From - To)	
4. TITLE AND SUBTITLE Geometric Single-Qubit Quantum Gates for an Electron Spin in a Quantum Dot			5a. CONTRACT NUMBER		
			5b. GRANT NUMBER		
			5c. PROGRAM ELEMENT NUMBER		
6. AUTHOR(S) Vladimir S. Malinovsky and Sergey Rudin			5d. PROJECT NUMBER		
			5e. TASK NUMBER		
			5f. WORK UNIT NUMBER		
7. PERFORMING ORGANIZATION NAME(S) AND ADDRESS(ES) U.S. Army Research Laboratory ATTN: RDRL-SEE-M Adelphi, MD 20783-1197			8. PERFORMING ORGANIZATION REPORT NUMBER ARL-TR-6641		
9. SPONSORING/MONITORING AGENCY NAME(S) AND ADDRESS(ES)			10. SPONSOR/MONITOR'S ACRONYM(S)		
			11. SPONSOR/MONITOR'S REPORT NUMBER(S)		
12. DISTRIBUTION/AVAILABILITY STATEMENT Approved for public release; distribution is unlimited.					
13. SUPPLEMENTARY NOTES					
14. ABSTRACT We propose a scheme to perform arbitrary unitary operations on a single electron-spin qubit in a quantum dot. The design is solely based on the geometrical phase that the qubit state acquires after a cyclic evolution in the parameter space. The scheme uses ultrafast linearly chirped pulses providing adiabatic excitation of the qubit states and the geometric phase is fully controlled by the relative phase between pulses. The analytic expression of the evolution operator for the electron spin in a quantum dot, which provides a clear geometrical interpretation of the qubit dynamics, is obtained. Using parameters of indium gallium nitride (InGaN)/gallium nitride (GaN), GaN/aluminum nitride (AlN) quantum dots, we provide an estimate for the time scale of the qubit rotations and parameters of the external fields.					
15. SUBJECT TERMS electron spin qubit, quantum gates					
16. SECURITY CLASSIFICATION OF:			17. LIMITATION OF ABSTRACT UU	18. NUMBER OF PAGES 44	19a. NAME OF RESPONSIBLE PERSON Vladimir S. Malinovsky
a. REPORT Unclassified	b. ABSTRACT Unclassified	c. THIS PAGE Unclassified			19b. TELEPHONE NUMBER (Include area code) 301-394-0422

---

## Contents

---

<b>List of Figures</b>	<b>v</b>
<b>1. Introduction</b>	<b>1</b>
<b>2. General Equations of Motion</b>	<b>1</b>
<b>3. Non-Impulsive Case</b>	<b>6</b>
<b>4. Adiabatic Solution</b>	<b>6</b>
<b>5. Bloch Vector Representation</b>	<b>10</b>
<b>6. Alternative Derivation of the Bloch Equation</b>	<b>13</b>
<b>7. Evolution Operator of the Bloch Vector</b>	<b>16</b>
<b>8. Ultrafast Qubit Rotations Using Geometrical Phase</b>	<b>18</b>
<b>9. Rotation in the Bloch Representation</b>	<b>21</b>
<b>10. Generalization of the Single-Qubit Operation Using Bright-Dark Basis</b>	<b>23</b>
<b>11. Electron Spin in a Quantum Dot as a Qubit</b>	<b>26</b>
<b>12. Conclusion</b>	<b>29</b>
<b>13. References</b>	<b>30</b>

**Appendix. Eigenvectors of the Pauli matrices** **33**

**Distribution List** **35**

---

## List of Figures

---

Figure 1. Energy structure of the three-level system comprised of the two electron spin states and the trion state. ....	2
Figure 2. The density plot of the $ 1\rangle$ state population (a) and coherence (b) as a function of the effective pulse area and frequency chirp; $\alpha_P = \alpha_S$ , $\delta = 0$ . Initially, only the $ 1\rangle$ state is populated.....	9
Figure 3. The density plot of the $ 1\rangle$ state population (a) and coherence (b) as a function of the effective pulse area and frequency chirp; $\alpha_P = \alpha_S$ , $\delta\tau_0 = 0.75$ . Initially, only the $ 1\rangle$ state is populated.....	10
Figure 4. The Bloch vector representation of the qubit state. Excitation of the qubit by an external field corresponds to the rotation of the $\mathbf{B}$ vector about the pseudo field vector, $\mathbf{\Omega}$ , with components determined by the effective Rabi frequency $\Omega_e(t)$ , detuning $\delta$ , and the relative phase $\Delta\phi$ . ....	11
Figure 5. The Bloch vector trajectory for the qubit state $ 0\rangle$ in panel (a) and the qubit state $ 1\rangle$ in panel (b) generated by the sequence of two $\pi$ -pulses with the relative phase $\varphi + \pi$ . .	19
Figure 6. The Bloch vector trajectory for the qubit state $ i\rangle$ in panel (a) and the qubit state $ -i\rangle$ in panel (b) generated by the sequence of two $\pi/2$ -pulses and one $\pi$ pulse with the relative phase $\varphi + \pi$ . ....	20
Figure 7. Optical selection rules in different bases.....	27
Figure 8. The population dynamics of the resonant qubit states with (dotted lines) and without (solid lines) adiabatic elimination of the trion state in the three-level system. The excitation is generated by the sequence of two pairs of $\pi$ -pulses (Gaussian pulse envelopes) with the relative phase $\Delta\varphi = \pi/2$ . ....	28

INTENTIONALLY LEFT BLANK.

---

## 1. Introduction

---

The electron spin in a single quantum dot is one of the perspective realizations of a qubit for the implementation of a quantum computer. During the last decade several control schemes to perform single gate operations on a single quantum dot spin have been reported (1–4). Here we propose a scheme that allows performing ultrafast arbitrary unitary operations on a single qubit represented by the electron spin. The idea of geometric manipulation of the qubit wave function has been recently developed into a new research direction called geometric quantum computing (15–17). The main motivation of this development is the robustness of geometric quantum gates against noise (15, 18, 19). In this report, we demonstrate how to use the geometric phase, which the Bloch vector gains along the cyclic path, to prepare an arbitrary state of a single qubit. We show that the geometrical phase is fully controllable by the relative phase between the external fields. Realistic implementation of the proposed design using the electron spin in a charged quantum dot as an example of a qubit is discussed.

---

## 2. General Equations of Motion

---

Let us consider the coherent Raman excitation in the three-level  $\Lambda$ -type system consisting of the two lowest states of electron spin  $|0\rangle \equiv |-X\rangle$  and  $|1\rangle \equiv |X\rangle$  coupled through an intermediate trion state  $|T\rangle$  consisting of two electrons and a heavy hole (5) (figure 1). We assume that the trion state is far off-resonance with the external fields to ensure that decoherence on the trion-qubit transitions can be neglected. The electron spin states are split by an external magnetic field; the separation energy is  $\hbar\omega_e$ . The total wave function of the system

$$|\Psi(t)\rangle = a_0(t)|0\rangle + a_1(t)|1\rangle + b(t)|T\rangle, \quad (1)$$

where  $a_{0,1}(t)$  and  $b(t)$  are the probability amplitudes, is governed by the time-dependent Schrödinger equation with the Hamiltonian

$$\mathbf{H} = \hbar \begin{pmatrix} 0 & 0 & -(\Omega_P(t) + \bar{\Omega}_S(t)) \\ 0 & \omega_e & -(\bar{\Omega}_P(t) + \Omega_S(t)) \\ -(\Omega_P(t) + \bar{\Omega}_S(t)) & -(\bar{\Omega}_P(t) + \Omega_S(t)) & \omega_T \end{pmatrix}, \quad (2)$$

where  $\Omega_{P,S}(t) = \Omega_{P0,S0}(t) \cos[\omega_{P,S}t + \phi_{P,S}(t)]$ ,  $\bar{\Omega}_{P,S}(t) = \bar{\Omega}_{P0,S0}(t) \cos[\omega_{P,S}t + \phi_{P,S}(t)]$ ,

$\Omega_{P0,S0}(t) = \mu_{0T,T1}E_{P,S}(t)/\hbar$ , and  $\bar{\Omega}_{P0,S0}(t) = \mu_{1T,T0}E_{P,S}(t)/\hbar$  are the Rabi frequencies,  $\mu_{0T,T1}$  are the dipole moments,  $E_{P,S}(t)$  are the pulse envelopes,  $\omega_{P,S}$  are the center frequencies,  $\phi_{P,S}(t)$  are the time-dependent phases, and  $\hbar\omega_T$  is the energy of the trion state.

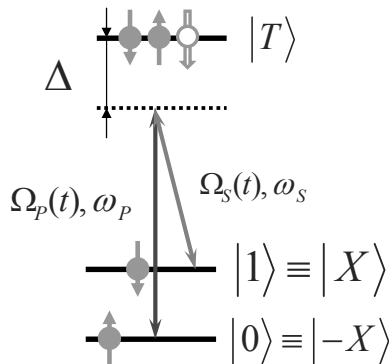


Figure 1. Energy structure of the three-level system comprised of the two electron spin states and the trion state.

We are considering here a case of linearly chirped pulses such that

$$\phi_{P,S}(t) = \phi_{P,S} + \alpha_{P,S}t^2/2, \quad (3)$$

where  $\phi_{P,S}$  are the initial phases and  $\alpha_{P,S}$  are the chirps of the pulses.

Using transformation  $|\Psi(t)\rangle = \mathbf{U}_{RWA}|\tilde{\Psi}(t)\rangle$ , where

$$\mathbf{U}_{RWA} = \begin{pmatrix} 1 & 0 & 0 \\ 0 & e^{i(\omega_S - \omega_P)t} & 0 \\ 0 & 0 & e^{-i\omega_P t} \end{pmatrix}, \quad (4)$$

$$\mathbf{U}_{RWA}^{-1} = \begin{pmatrix} 1 & 0 & 0 \\ 0 & e^{-i(\omega_S - \omega_P)t} & 0 \\ 0 & 0 & e^{i\omega_P t} \end{pmatrix}, \quad (5)$$

we make the rotating wave approximation (RWA) by neglecting the rapidly oscillating terms with

frequency  $2\omega_S$ ,  $2\omega_P$  and  $\omega_S + \omega_P$ . In the RWA, the Hamiltonian has the following form

$$\begin{aligned}
\tilde{\mathbf{H}} &= \mathbf{U}_{RWA}^{-1} \mathbf{H} \mathbf{U}_{RWA} - i\hbar \mathbf{U}_{RWA}^{-1} \dot{\mathbf{U}}_{RWA} \\
&= -\frac{\hbar}{2} \begin{pmatrix} 0 & 0 & \Omega_{P+} + \bar{\Omega}_{S+} e^{-i\Delta\omega t} \\ 0 & -2\omega_e & \bar{\Omega}_{P+}(t) e^{i\Delta\omega t} + \Omega_{S+} \\ \Omega_{P+}^* + \bar{\Omega}_{S+}^* e^{i\Delta\omega t} & \bar{\Omega}_{P+}^* e^{-i\Delta\omega t} + \Omega_{S+}^* & -2\omega_T \end{pmatrix} \\
&\quad + \hbar \begin{pmatrix} 0 & 0 & 0 \\ 0 & -\Delta\omega & 0 \\ 0 & 0 & -\omega_P \end{pmatrix} \\
&= -\frac{\hbar}{2} \begin{pmatrix} 0 & 0 & \Omega_{P+} + \bar{\Omega}_{S+} e^{-i\Delta\omega t} \\ 0 & 2(\Delta\omega - \omega_e) & \bar{\Omega}_{P+}(t) e^{i\Delta\omega t} + \Omega_{S+} \\ \Omega_{P+}^* + \bar{\Omega}_{S+}^* e^{i\Delta\omega t} & \bar{\Omega}_{P+}^* e^{-i\Delta\omega t} + \Omega_{S+}^* & -2\Delta_P \end{pmatrix}, \quad (6)
\end{aligned}$$

where  $\Delta_P = \omega_T - \omega_P$ ,  $\Delta\omega = \omega_P - \omega_S$ ,  $\Omega_{P+} = \Omega_{P0}(t) e^{i\phi_P(t)}$ ,  $\Omega_{S+} = \Omega_{S0}(t) e^{i\phi_S(t)}$ ,  $\bar{\Omega}_{P+} = \bar{\Omega}_{P0}(t) e^{i\phi_P(t)}$ ,  $\bar{\Omega}_{S+} = \bar{\Omega}_{S0}(t) e^{i\phi_S(t)}$ .

Assuming large detunings of the pump and Stokes field frequencies from the transition frequencies to the trion state, we apply the adiabatic elimination of the trion state. In that case,  $\dot{\tilde{b}} \approx 0$  and we find

$$\tilde{b} = \frac{1}{2\Delta_P} [(\Omega_{P+}^* + \bar{\Omega}_{S+}^* e^{i\Delta\omega t}) \tilde{a}_0(t) + (\bar{\Omega}_{P+}^* e^{-i\Delta\omega t} + \Omega_{S+}^*) \tilde{a}_1(t)]. \quad (7)$$

Substituting equation 7 into equations for  $a_{0,1}$  after some algebra, we obtain the following form of the Hamiltonian for the effective two-level system

$$\tilde{\mathbf{H}} = -\frac{\hbar}{2} \begin{pmatrix} \Omega_{ac0}(t) & \Omega_{eff}(t) \\ \Omega_{eff}^*(t) & \Omega_{ac1}(t) - 2\delta \end{pmatrix}, \quad (8)$$

where  $\delta = \omega_e - \Delta\omega$ ,

$$\Omega_{ac0}(t) = \frac{1}{2\Delta_P} (\Omega_{P0}^2(t) + \bar{\Omega}_{S0}^2(t) + 2\Omega_{P0}(t) \bar{\Omega}_{S0}(t) \cos[\phi_P(t) - \phi_S(t) + \Delta\omega t]), \quad (9)$$

$$\Omega_{ac1}(t) = \frac{1}{2\Delta_P} (\Omega_{S0}^2(t) + \bar{\Omega}_{P0}^2(t) + 2\Omega_{S0}(t) \bar{\Omega}_{P0}(t) \cos[\phi_P(t) - \phi_S(t) + \Delta\omega t]), \quad (10)$$

$$\begin{aligned}\Omega_{eff}(t) = & \frac{e^{-i\Delta\omega t}}{2\Delta_P} (\Omega_{P0}(t)\bar{\Omega}_{P0}(t) + \Omega_{S0}(t)\bar{\Omega}_{S0}(t) \\ & + \Omega_{P0}(t)\Omega_{S0}(t)e^{i[\phi_P(t)-\phi_S(t)+\Delta\omega t]} + \bar{\Omega}_{P0}(t)\bar{\Omega}_{S0}(t)e^{-i[\phi_P(t)-\phi_S(t)+\Delta\omega t]}) .\end{aligned}\quad (11)$$

Since  $\Omega_{P0}(t)\Omega_{S0}(t) = \bar{\Omega}_{P0}(t)\bar{\Omega}_{S0}(t)$ , we have

$$\begin{aligned}\Omega_{eff}(t) = & \frac{e^{-i\Delta\omega t}}{2\Delta_P} (\Omega_{P0}(t)\bar{\Omega}_{P0}(t) + \Omega_{S0}(t)\bar{\Omega}_{S0}(t) \\ & + 2\Omega_{P0}(t)\Omega_{S0}(t) \cos[\phi_P(t) - \phi_S(t) + \Delta\omega t]) .\end{aligned}\quad (12)$$

Making the transformation  $|\tilde{\Psi}(t)\rangle = \mathcal{U}|\bar{\Psi}(t)\rangle$ , with

$$\mathcal{U} = \begin{pmatrix} e^{-i\delta t/2+i\int_{-\infty}^t dt'\Omega_{st}(t')} & 0 \\ 0 & e^{-i\delta t/2+i\int_{-\infty}^t dt'\Omega_{st}(t')} \end{pmatrix} = e^{-i\delta t/2+i\int_{-\infty}^t dt'\Omega_{st}(t')} \mathbf{I}, \quad (13)$$

where  $\Omega_{st}(t) = (\Omega_{ac0}(t) + \Omega_{ac1}(t))/4$ , we can rewrite equation 8 in more symmetric form. In the new basis, the Hamiltonian takes the form

$$\begin{aligned}\bar{\mathbf{H}} = & \mathcal{U}^{-1}\tilde{\mathbf{H}}\mathcal{U} - i\hbar\mathcal{U}^{-1}\dot{\mathcal{U}} = \tilde{\mathbf{H}} + \hbar(\Omega_{st}(t) - \delta/2)\mathbf{I} \\ = & -\frac{\hbar}{2} \begin{pmatrix} \delta + \Omega_{dif}(t) & \Omega_{eff}(t) \\ \Omega_{eff}^*(t) & -\delta - \Omega_{dif}(t) \end{pmatrix},\end{aligned}\quad (14)$$

where  $\Omega_{dif}(t) = (\Omega_{ac0}(t) - \Omega_{ac1}(t))/2$ .

Taking into account the exact time-dependence of the phases in equation 3 we apply another transformation  $|\bar{\Psi}(t)\rangle = \mathcal{U}_F|\check{\Psi}(t)\rangle$ , with

$$\mathcal{U}_F = \begin{pmatrix} e^{i\zeta t^2/4} & 0 \\ 0 & e^{-i\zeta t^2/4} \end{pmatrix} = e^{i\zeta\frac{t^2}{4}\sigma_z}, \quad (15)$$

where  $\zeta = \alpha_P - \alpha_S$ . Therefore, in the field interaction representation the Hamiltonian takes the

following form

$$\begin{aligned}
\check{\mathbf{H}} &= \mathcal{U}_F^{-1} \bar{\mathbf{H}} \mathcal{U}_F - i\hbar \mathcal{U}_F^{-1} \dot{\mathcal{U}}_F \\
&= -\frac{\hbar}{2} \begin{pmatrix} \delta + \Omega_{dif}(t) & \Omega_{eff}(t)e^{-i\zeta t^2/4} \\ \Omega_{eff}^*(t)e^{i\zeta t^2/4} & -\delta - \Omega_{dif}(t) \end{pmatrix} + \frac{\hbar}{2} \begin{pmatrix} \zeta t & 0 \\ 0 & -\zeta t \end{pmatrix} \\
&= -\frac{\hbar}{2} \begin{pmatrix} \delta - \zeta t + \Omega_{dif}(t) & \Omega_{eff}(t)e^{-i\zeta t^2/4} \\ \Omega_{eff}^*(t)e^{i\zeta t^2/4} & -\delta + \zeta t - \Omega_{dif}(t) \end{pmatrix} \\
&= -\frac{\hbar}{2} \begin{pmatrix} \delta(t) & \bar{\Omega}_{eff}(t)e^{i\Delta\phi} \\ \bar{\Omega}_{eff}^*(t)e^{-i\Delta\phi} & -\delta(t) \end{pmatrix}, \tag{16}
\end{aligned}$$

where  $\delta(t) = \delta + (\alpha_S - \alpha_P)t + \Omega_{dif}(t)$ ,  $\Delta\phi = \phi_P - \phi_S$ ,

$$\begin{aligned}
\bar{\Omega}_{eff}(t) &= \frac{\Omega_{P0}(t)\Omega_{S0}(t)}{2\Delta_P} \left( 1 + \frac{\Omega_{P0}(t)\bar{\Omega}_{P0}(t) + \Omega_{S0}(t)\bar{\Omega}_{S0}(t)}{\Omega_{P0}(t)\Omega_{S0}(t)} e^{-i[\Delta\phi + \Delta\omega t + \zeta t^2/2]} \right. \\
&\quad \left. + \frac{\bar{\Omega}_{P0}(t)\bar{\Omega}_{S0}(t)}{\Omega_{P0}(t)\Omega_{S0}(t)} e^{-2i[\Delta\phi + \Delta\omega t + \zeta t^2/2]} \right). \tag{17}
\end{aligned}$$

In general, the differential AC Stark shift,  $\Omega_{dif}(t)$  is not zero and has to be taken into account.

Using the definition of the Rabi frequency, we can rewrite equations 9 and 10 in the form

$$\Omega_{ac0}(t) = \frac{\mu_{0T}^2}{2\hbar^2\Delta_P} (E_P^2(t) + E_S^2(t) + 2E_P(t)E_S(t) \cos[\phi_P(t) - \phi_S(t) + \Delta\omega t]), \tag{18}$$

$$\Omega_{ac1}(t) = \frac{\mu_{1T}^2}{2\hbar^2\Delta_P} (E_P^2(t) + E_S^2(t) + 2E_P(t)E_S(t) \cos[\phi_P(t) - \phi_S(t) + \Delta\omega t]). \tag{19}$$

In the case, when  $\mu_{0T} \approx \mu_{1T}$ , the AC Stark shifts are the same for both qubit states, so that  $\Omega_{dif}(t) = 0$ , and we have

$$\check{\mathbf{H}} = -\frac{\hbar}{2} \begin{pmatrix} \delta - \zeta t & \bar{\Omega}_{eff}(t)e^{i\Delta\phi} \\ \bar{\Omega}_{eff}^*(t)e^{-i\Delta\phi} & -\delta + \zeta t \end{pmatrix}. \tag{20}$$

Note that we do not require completely overlapped pulses here.

---

### 3. Non-Impulsive Case

---

In some excitation schemes, due to selection rules that take into consideration the polarization of the external field, the pump and Stokes field interact only with the corresponding transitions and the general Hamiltonian can be simplified. For that case, we can obtain the correct form of the Hamiltonian by putting  $\bar{\Omega}_{P0}(t) = \bar{\Omega}_{S0}(t) = 0$  in equations 9, 10 and 17. It results in

$$\Omega_{ac0}(t) = \frac{1}{2\Delta_P} \Omega_{P0}^2(t), \quad (21)$$

$$\Omega_{ac1}(t) = \frac{1}{2\Delta_P} \Omega_{S0}^2(t), \quad (22)$$

$$\Omega_{dif}(t) = \frac{1}{4\Delta_P} [\Omega_{P0}^2(t) - \Omega_{S0}^2(t)], \quad (23)$$

$$\bar{\Omega}_{eff}(t) = \frac{\Omega_{P0}(t)\Omega_{S0}(t)}{2\Delta_P}. \quad (24)$$

Therefore, in the field interaction representation, the Hamiltonian has the form

$$\check{H} = -\frac{\hbar}{2} \begin{pmatrix} \delta(t) & \bar{\Omega}_{eff}(t)e^{i\Delta\phi} \\ \bar{\Omega}_{eff}^*(t)e^{-i\Delta\phi} & -\delta(t) \end{pmatrix}, \quad (25)$$

where

$$\delta(t) = \delta + (\alpha_S - \alpha_P)t + [\Omega_{P0}^2(t) - \Omega_{S0}^2(t)]/4\Delta_P. \quad (26)$$


---

### 4. Adiabatic Solution

---

The Hamiltonian in equation 25 controls the dynamics of the qubit wave function in the approximation of the adiabatic elimination of the trion state. Here we consider the adiabatic excitation of the qubit and find the adiabatic solution of the Schrödinger equation with the Hamiltonian in equation 25.

Since the phase factor,  $e^{i\Delta\phi}$ , of the coupling term in equation 25 is time independent, it is

convenient to use the following transformation  $|\Phi(t)\rangle = \mathbf{A}|\Psi(t)\rangle$ , where

$$\mathbf{A} = |0\rangle\langle 0| + e^{i\Delta\phi}|1\rangle\langle 1| = e^{i\Delta\phi/2}e^{-i\Delta\phi\sigma_z/2}, \quad (27)$$

so that the new wave function is governed by the Hamiltonian

$$\begin{aligned} \bar{\mathbf{H}} &= \mathbf{A}\check{\mathbf{H}}\mathbf{A}^{-1} = -\frac{\hbar}{2} \begin{pmatrix} \delta(t) & \Omega_e(t) \\ \Omega_e(t) & -\delta(t) \end{pmatrix} \\ &= -\frac{\hbar}{2} (\delta(t)\sigma_z + \Omega_e(t)\sigma_x). \end{aligned} \quad (28)$$

To solve the Schrödinger equation in the adiabatic representation, we apply another transformation:  $|\bar{\Phi}(t)\rangle = \mathbf{R}(t)|\Phi(t)\rangle$ , where

$$\mathbf{R}(t) = \begin{pmatrix} \cos \theta(t) & \sin \theta(t) \\ -\sin \theta(t) & \cos \theta(t) \end{pmatrix} = e^{i\theta(t)\sigma_y}, \quad (29)$$

and  $\tan[2\theta(t)] = \Omega_e(t)/\delta(t)$ . In the new basis the Hamiltonian, equation 28, takes the form

$$\begin{aligned} \tilde{\mathbf{H}}(t) &= \mathbf{R}(t)\bar{\mathbf{H}}(t)\mathbf{R}^{-1}(t) \\ &= \begin{pmatrix} -\frac{\hbar}{2}\sqrt{\delta^2(t) + \Omega_e^2(t)} & 0 \\ 0 & \frac{\hbar}{2}\sqrt{\delta^2(t) + \Omega_e^2(t)} \end{pmatrix} \\ &= -\hbar\lambda(t)\sigma_z/2, \end{aligned} \quad (30)$$

where  $\lambda(t) = \sqrt{\delta^2(t) + \Omega_e^2(t)}$ .

As we see, the Hamiltonian in equation 30 is diagonal in the adiabatic basis and we can readily write down the solution. However, since the transformation  $\mathbf{R}(t)$  is time dependent, an additional nonadiabatic coupling term is present in the general Schrödinger equation

$$i\hbar|\dot{\bar{\Phi}}(t)\rangle = -\frac{1}{2}\hbar\lambda(t)\sigma_z|\bar{\Phi}(t)\rangle - \hbar\dot{\theta}(t)\sigma_y|\bar{\Phi}(t)\rangle, \quad (31)$$

where

$$\dot{\theta}(t) = -\frac{\Omega_e(t)\dot{\delta}(t) - \delta(t)\dot{\Omega}_e(t)}{2(\Omega_e^2(t) + \delta^2(t))}. \quad (32)$$

Neglecting the nonadiabatic coupling term in equation 31, we readily obtain for the qubit wave

function in the original basis

$$|\Psi(t)\rangle = e^{i\frac{\Delta\phi}{2}\sigma_z} e^{-i\theta(t)\sigma_y} e^{i\frac{\Lambda(t)}{2}\sigma_z} e^{i\theta(0)\sigma_y} e^{-i\frac{\Delta\phi}{2}\sigma_z} |\Psi(0)\rangle. \quad (33)$$

where  $\Lambda(t) = \int_0^t dt' \lambda(t')$ . Note, that the general form of the evolution operator in equation 33 is well justified if the following condition  $|\Omega_e(t)\dot{\delta}(t) - \dot{\Omega}_e(t)\delta(t)| \ll \lambda^3(t)$  is valid.

In the case of completely overlapped pulses,  $\Omega_{P0}(t) = \Omega_{S0}(t)$ , with identical chirp rates,  $\alpha_P = \alpha_S$ , for the resonant qubit,  $\delta(t) = \delta = 0$ , we have  $\theta(t) = \theta(0) = \pi/4$  and the transformation matrix becomes  $\mathbf{R}(t) = \mathbf{R}(0) = e^{i\pi\sigma_y/4}$ . Therefore, the unitary evolution operator for the wave function of the resonant qubit takes the form

$$\begin{aligned} \mathbf{U}(t) &= \begin{pmatrix} \cos(S(t)/2) & ie^{i\Delta\phi} \sin(S(t)/2) \\ ie^{-i\Delta\phi} \sin(S(t)/2) & \cos(S(t)/2) \end{pmatrix} \\ &= \cos(S(t)/2) \mathbf{I} + i \sin(S(t)/2) (e^{i\Delta\phi} \boldsymbol{\sigma}_+ + e^{-i\Delta\phi} \boldsymbol{\sigma}_-) \\ &= \cos(S(t)/2) \mathbf{I} - i \sin(S(t)/2) (\mathbf{n} \cdot \boldsymbol{\sigma}) = e^{-iS(t)\mathbf{n}\cdot\boldsymbol{\sigma}/2}, \end{aligned} \quad (34)$$

where  $S(t) = \int_0^t dt' \Omega_e(t')$  is the effective pulse area,  $\mathbf{n} = (-\cos \Delta\phi, \sin \Delta\phi, 0)$ ,  $\boldsymbol{\sigma}_\pm = (\boldsymbol{\sigma}_x \pm i\boldsymbol{\sigma}_y)/2$  are the Pauli raising and lowering operators, and  $\boldsymbol{\sigma}_{x,y,z}$  are the Pauli operators. Note, that the nonadiabatic coupling term, equation 32, is zero for the resonant qubit and the solution of the Schrödinger equation in the adiabatic approximation, equation 34, is the exact solution.

The density plots of the population and coherence ( $|a_0(T)a_1^*(T)|$ ) at the final time (after the pulse excitation) as a function of the effective pulse area,  $S(T)$ , and the dimensionless frequency chirp parameter,  $\alpha'/\tau_0^2$ , described by the unitary evolution operator in equation 34 is depicted in figure 2. We use the Gaussian shape for the pulse envelopes, assuming that linear chirp is obtained by applying a linear optics technique, meaning that a transform-limited pulse of duration  $\tau_0$  is chirped, conserving the energy of the pulse (6, 7). The temporal ( $\alpha$ ) and spectral ( $\alpha'$ ) chirps are related as  $\alpha = \alpha' \tau_0^{-4} / (1 + \alpha'^2 / \tau_0^4)$  (6, 7), where  $\tau_0$  is the transform-limited pulse duration. We observe the Rabi oscillation regime, when the population of the qubit states is changing between 0 and 1 while the coherence is changing between 0 and 1/2. This behavior does not depend on the chirp rate, since the effective Rabi frequency  $\Omega_e(t)$  is determined by the product of the pump and Stokes Rabi frequencies:  $\Omega_{P0,S0}(t) = \Omega_0 \exp\{-t^2/(2\tau^2)\} / [1 + \alpha'^2/\tau_0^4]^{1/4}$  with the chirp-dependent pulse duration  $\tau = \tau_0 [1 + \alpha'^2/\tau_0^4]^{1/2}$  and the amplitude (6, 7).

In turn, for the off-resonant qubits,  $\delta \neq 0$ , the evolution operator in the adiabatic approximation

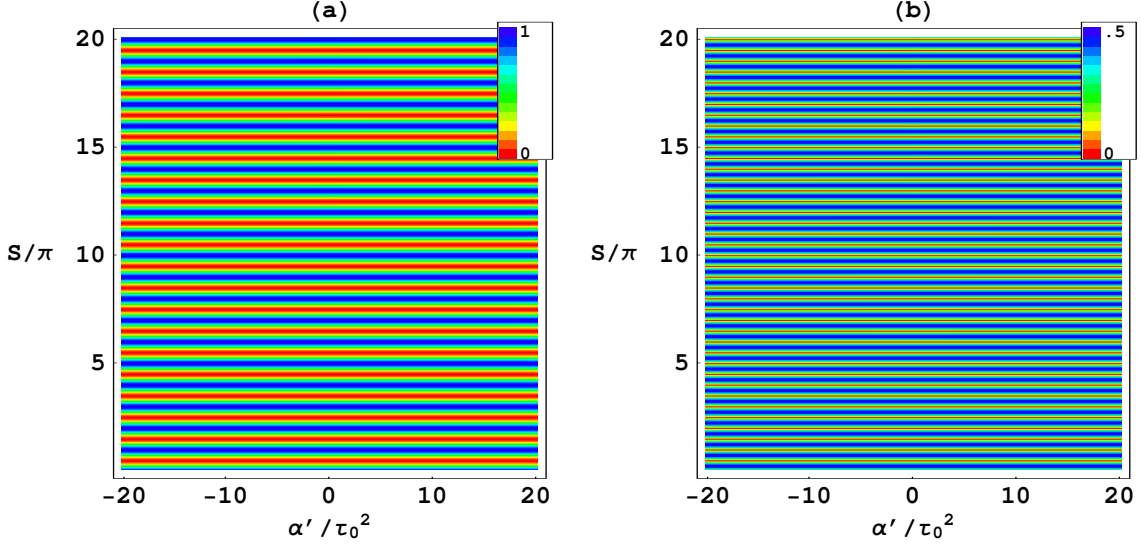


Figure 2. The density plot of the  $|1\rangle$  state population (a) and coherence (b) as a function of the effective pulse area and frequency chirp;  $\alpha_P = \alpha_S$ ,  $\delta = 0$ . Initially, only the  $|1\rangle$  state is populated.

takes the form

$$U(t) = \begin{pmatrix} e^{i\xi(t)} \cos \theta(t) & -e^{-i\xi(t)} e^{i\Delta\phi} \sin \theta(t) \\ e^{i\xi(t)} e^{-i\Delta\phi} \sin \theta(t) & e^{-i\xi(t)} \cos \theta(t) \end{pmatrix}, \quad (35)$$

where

$$\cos \theta(t) = \frac{1}{\sqrt{2}} \sqrt{1 + \frac{\delta}{\sqrt{\delta^2 + \Omega_e^2(t)}}}, \quad (36a)$$

$$\sin \theta(t) = \frac{1}{\sqrt{2}} \sqrt{1 - \frac{\delta}{\sqrt{\delta^2 + \Omega_e^2(t)}}} \quad (36b)$$

and  $\xi(t) = \frac{1}{2} \int_0^t \sqrt{\delta^2 + \Omega_e^2(t')} dt'$  is the effective pulse area.

Note that for the off-resonant case the transformation matrixes are

$$\begin{aligned} \mathbf{R}^{-1}(t) &= \begin{pmatrix} \cos \theta(t) & -\sin \theta(t) \\ \sin \theta(t) & \cos \theta(t) \end{pmatrix}, \\ \mathbf{R}(0) &= \begin{pmatrix} 1 & 0 \\ 0 & 1 \end{pmatrix}. \end{aligned} \quad (37)$$

Figure 3 demonstrates excitation of the off-resonant qubit. As expected, the population of the

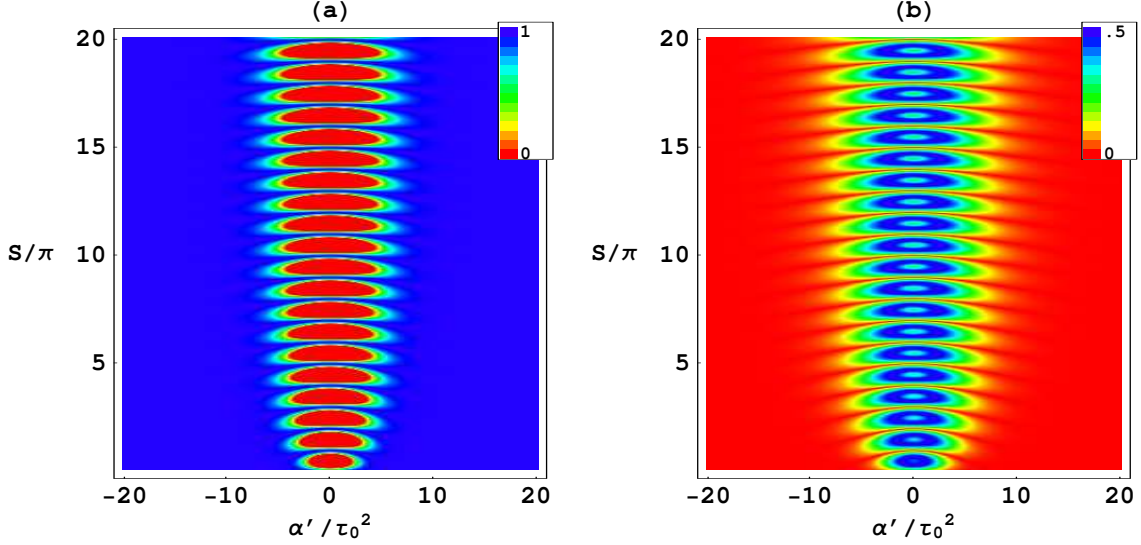


Figure 3. The density plot of the  $|1\rangle$  state population (a) and coherence (b) as a function of the effective pulse area and frequency chirp;  $\alpha_P = \alpha_S$ ,  $\delta\tau_0 = 0.75$ . Initially, only the  $|1\rangle$  state is populated.

off-resonant qubit at the final time is not changed by the external fields as long as the pulse excitation parameters are in the adiabatic regime. This is the regime of adiabatic return. However, we still observe the Rabi oscillation for the value of the chirp  $|\alpha'| \lesssim 5\tau_0^2$ . This is the area of nonadiabatic population transfer where the nonadiabatic coupling term cannot be neglected in equation 31.

---

## 5. Bloch Vector Representation

---

The dynamics of the qubit wave function can be described equally well using the Bloch vector representation. In addition, the Bloch vector formalism allows a very nice and clear geometrical interpretation of qubit dynamics (8). In this section, we give a short overview of the Bloch picture.

A general state of a qubit can be described as

$$|\Psi\rangle = a_0(t)|0\rangle + a_1(t)|1\rangle = \cos(\beta/2)|0\rangle + e^{i\alpha}\sin(\beta/2)|1\rangle, \quad (38)$$

where  $\alpha$  and  $\beta$  are the phase parameters. Up to an insignificant global phase, the wave function

can be mapped into a unitary Bloch vector  $\mathbf{B} = (u, v, w)$ , as shown in figure 4.

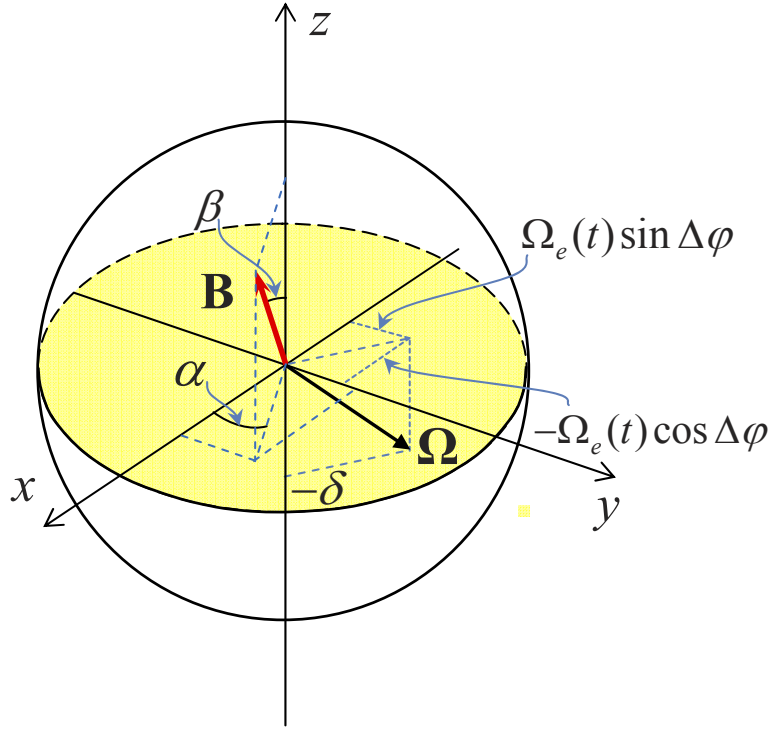


Figure 4. The Bloch vector representation of the qubit state. Excitation of the qubit by an external field corresponds to the rotation of the  $\mathbf{B}$  vector about the pseudo field vector,  $\mathbf{\Omega}$ , with components determined by the effective Rabi frequency  $\Omega_e(t)$ , detuning  $\delta$ , and the relative phase  $\Delta\phi$ .

To use Bloch vector representation, we construct the qubit density matrix

$$\rho = |\Psi\rangle\langle\Psi| = \begin{pmatrix} \rho_{00} & \rho_{01} \\ \rho_{10} & \rho_{11} \end{pmatrix} = \frac{1}{2} \begin{pmatrix} 1 + \cos\beta & e^{-i\alpha} \sin\beta \\ e^{i\alpha} \sin\beta & 1 - \cos\beta \end{pmatrix}, \quad (39)$$

where  $\rho_{ij} = a_i(t)a_j^*(t)$ ,  $i, j = 0, 1$ . Using a Pauli matrix decomposition

$$\begin{aligned} \rho &= \frac{1}{2} (\mathbf{I} + \mathbf{B} \cdot \vec{\sigma}) \\ &= \frac{1}{2} (\mathbf{I} + u \cdot \sigma_x + v \cdot \sigma_y + w \cdot \sigma_z) \\ &= \frac{1}{2} (\mathbf{I} + \cos\alpha \sin\beta \cdot \sigma_x + \sin\alpha \sin\beta \cdot \sigma_y + \cos\beta \cdot \sigma_z), \end{aligned} \quad (40)$$

we identify relation between the components of the qubit wave function, the qubit density matrix

elements, and the Bloch vector components. Therefore, we obtain the following expression

$$\mathbf{B} = \begin{pmatrix} u \\ v \\ w \end{pmatrix} = \begin{pmatrix} \varrho_{01} + \varrho_{10} \\ i(\varrho_{01} - \varrho_{10}) \\ \varrho_{00} - \varrho_{11} \end{pmatrix} = \begin{pmatrix} \cos \alpha \sin \beta \\ \sin \alpha \sin \beta \\ \cos \beta \end{pmatrix}. \quad (41)$$

Taking into account the Hamiltonian in equation 25, the equation of motion for the density matrix  $i\hbar\dot{\boldsymbol{\rho}} = \mathbf{H}\boldsymbol{\rho} - \boldsymbol{\rho}\mathbf{H}$  takes the following explicit form

$$i\dot{\varrho}_{00} = (e^{-i\Delta\phi}\varrho_{01} - e^{i\Delta\phi}\varrho_{10})\Omega_e(t)/2, \quad (42a)$$

$$i\dot{\varrho}_{01} = -\delta(t)\varrho_{01} - (\varrho_{11} - \varrho_{00})\Omega_e(t)e^{i\Delta\phi}/2, \quad (42b)$$

$$i\dot{\varrho}_{10} = \delta(t)\varrho_{10} + (\varrho_{11} - \varrho_{00})\Omega_e(t)e^{-i\Delta\phi}/2, \quad (42c)$$

$$i\dot{\varrho}_{11} = -(e^{-i\Delta\phi}\varrho_{01} - e^{i\Delta\phi}\varrho_{10})\Omega_e(t)/2. \quad (42d)$$

Using the relations in equation 41, we can also write the dynamic equation in the Bloch vector representation as

$$\dot{u} = v\delta(t) + w\Omega_e(t)\sin\Delta\phi, \quad (43a)$$

$$\dot{v} = -u\delta(t) + w\Omega_e(t)\cos\Delta\phi, \quad (43b)$$

$$\dot{w} = -u\Omega_e(t)\sin\Delta\phi - v\Omega_e(t)\cos\Delta\phi. \quad (43c)$$

Introducing a pseudo field vector,  $\boldsymbol{\Omega}$ , with components determined by the effective Rabi frequency, two-photon detuning, and the relative phase between pump and Stokes pulses,

$$\boldsymbol{\Omega} = \begin{pmatrix} -\Omega_e(t)\cos\Delta\phi \\ \Omega_e(t)\sin\Delta\phi \\ -\delta(t) \end{pmatrix}, \quad (44)$$

we can rewrite equation 43 in the compact form

$$\dot{\mathbf{B}} = \boldsymbol{\Omega} \times \mathbf{B}. \quad (45)$$

This is the Bloch equation, which describes a precession of the Bloch vector,  $\mathbf{B}$ , about the pseudo field vector,  $\boldsymbol{\Omega}$ , and allows clear, intuitive interpretation of qubit dynamics.

---

## 6. Alternative Derivation of the Bloch Equation

---

As we showed in the previous section, the density matrix can be decomposed using Pauli matrixes as

$$\rho = \frac{1}{2} (\mathbf{I} + \mathbf{B} \cdot \vec{\sigma}) . \quad (46)$$

It is also easy to verify that

$$\mathbf{B} = Tr[\vec{\sigma}\rho] = (Tr[\sigma_x\rho], Tr[\sigma_y\rho], Tr[\sigma_z\rho]) = (u, v, w) . \quad (47)$$

Using the Pauli matrix decomposition procedure  $Tr[\vec{\sigma}\mathbf{H}]$ , we can rewrite the Hamiltonian in equation 25 in the form

$$\mathbf{H} = \frac{\hbar}{2} (\boldsymbol{\Omega} \cdot \vec{\sigma}) , \quad (48)$$

where

$$\boldsymbol{\Omega} = (-\Omega_e(t) \cos \Delta\phi, \Omega_e(t) \sin \Delta\phi, -\delta(t)) . \quad (49)$$

Therefore, the equation of motion for the density matrix

$$\dot{\rho} = -\frac{i}{\hbar} (\mathbf{H}\rho - \rho\mathbf{H}) , \quad (50)$$

takes the form

$$\dot{\rho} = -\frac{i}{2} [(\boldsymbol{\Omega} \cdot \vec{\sigma}) \cdot \rho - \rho \cdot (\boldsymbol{\Omega} \cdot \vec{\sigma})] . \quad (51)$$

Using equation 46, we have

$$\begin{aligned} \dot{\rho} &= -\frac{i}{4} [(\boldsymbol{\Omega} \cdot \vec{\sigma}) \cdot (\mathbf{I} + \mathbf{B} \cdot \vec{\sigma}) - (\mathbf{I} + \mathbf{B} \cdot \vec{\sigma}) \cdot (\boldsymbol{\Omega} \cdot \vec{\sigma})] \\ &= -\frac{i}{4} [(\boldsymbol{\Omega} \cdot \vec{\sigma}) \cdot (\mathbf{B} \cdot \vec{\sigma}) - (\mathbf{B} \cdot \vec{\sigma}) \cdot (\boldsymbol{\Omega} \cdot \vec{\sigma})] . \end{aligned} \quad (52)$$

We know that for the two vectors  $\mathbf{M}$  and  $\mathbf{N}$  commuting with  $\vec{\sigma}$  (see, for example, equation 16.59 in reference (24))

$$(\mathbf{M} \cdot \vec{\sigma}) \cdot (\mathbf{N} \cdot \vec{\sigma}) = \mathbf{M} \cdot \mathbf{N} + i\vec{\sigma} \cdot (\mathbf{M} \times \mathbf{N}) . \quad (53)$$

Therefore,

$$\begin{aligned}
\dot{\rho} &= -\frac{i}{\hbar} (\mathbf{H}\rho - \rho\mathbf{H}) \\
&= -\frac{i}{4} [(\boldsymbol{\Omega} \cdot \vec{\sigma}) \cdot (\mathbf{B} \cdot \vec{\sigma}) - (\mathbf{B} \cdot \vec{\sigma}) \cdot (\boldsymbol{\Omega} \cdot \vec{\sigma})] \\
&= -\frac{i}{4} 2\vec{\sigma} \cdot (\boldsymbol{\Omega} \times \mathbf{B}) \\
&= \frac{1}{2} \vec{\sigma} \cdot (\boldsymbol{\Omega} \times \mathbf{B}), \tag{54}
\end{aligned}$$

and using equation 47, we obtain the Bloch equation

$$\dot{\mathbf{B}} = \text{Tr}[\vec{\sigma}\dot{\rho}] = \frac{1}{2} \text{Tr}[\vec{\sigma} \cdot \vec{\sigma} \cdot (\boldsymbol{\Omega} \times \mathbf{B})] = \boldsymbol{\Omega} \times \mathbf{B}. \tag{55}$$

Equation 55 can be written in the matrix form as

$$\dot{\mathbf{B}} = \mathbf{L}\mathbf{B}, \tag{56}$$

where

$$\mathbf{L} = \begin{pmatrix} 0 & \delta(t) & \Omega_e(t) \sin \Delta\phi \\ -\delta(t) & 0 & \Omega_e(t) \cos \Delta\phi \\ -\Omega_e(t) \sin \Delta\phi & -\Omega_e(t) \cos \Delta\phi & 0 \end{pmatrix}. \tag{57}$$

In the Bloch picture, the transformation of equation 27 is the rotation of the Bloch vector, so that the new Bloch vector is

$$\tilde{\mathbf{B}} = \begin{pmatrix} \tilde{u} \\ \tilde{v} \\ \tilde{w} \end{pmatrix} = \mathcal{R}\mathbf{B} = \begin{pmatrix} \cos \Delta\phi & -\sin \Delta\phi & 0 \\ \sin \Delta\phi & \cos \Delta\phi & 0 \\ 0 & 0 & 1 \end{pmatrix} \begin{pmatrix} u \\ v \\ w \end{pmatrix}. \tag{58}$$

That gives

$$\dot{\tilde{\mathbf{B}}} = \tilde{\boldsymbol{\Omega}} \times \tilde{\mathbf{B}} = \tilde{\mathbf{L}}\tilde{\mathbf{B}}, \tag{59}$$

where  $\tilde{\boldsymbol{\Omega}} = (\Omega_e(t), 0, -\delta(t))$ ,

$$\tilde{\mathbf{L}} = \mathcal{R}\mathbf{L}\mathcal{R}^{-1} = \begin{pmatrix} 0 & \delta(t) & 0 \\ -\delta(t) & 0 & \Omega_e(t) \\ 0 & -\Omega_e(t) & 0 \end{pmatrix}, \tag{60}$$

and

$$\mathcal{R}^{-1} = \begin{pmatrix} \cos \Delta\phi & \sin \Delta\phi & 0 \\ -\sin \Delta\phi & \cos \Delta\phi & 0 \\ 0 & 0 & 1 \end{pmatrix}. \quad (61)$$

The transformation  $R(t)$ , equation 30, in the Bloch picture is the rotation of the Bloch vector such that

$$\bar{\mathbf{B}} = \begin{pmatrix} \bar{u} \\ \bar{v} \\ \bar{w} \end{pmatrix} = \mathcal{R}_\theta \tilde{\mathbf{B}} = \begin{pmatrix} \cos[2\theta(t)] & 0 & -\sin[2\theta(t)] \\ 0 & 1 & 0 \\ \sin[2\theta(t)] & 0 & \cos[2\theta(t)] \end{pmatrix} \begin{pmatrix} \tilde{u} \\ \tilde{v} \\ \tilde{w} \end{pmatrix}, \quad (62)$$

where  $\tan[2\theta(t)] = \Omega_e(t)/\delta(t)$ .

It results in

$$\dot{\bar{\mathbf{B}}} = \bar{\mathbf{L}}\bar{\mathbf{B}} - \mathcal{R}_\theta \dot{\mathcal{R}}_\theta^{-1} \bar{\mathbf{B}}, \quad (63)$$

where

$$\bar{\mathbf{L}} = \mathcal{R}_\theta \tilde{\mathbf{L}} \mathcal{R}_\theta^{-1} = \begin{pmatrix} 0 & \lambda(t) & 0 \\ -\lambda(t) & 0 & 0 \\ 0 & 0 & 0 \end{pmatrix}, \quad (64)$$

and

$$\mathcal{R}_\theta^{-1} = \begin{pmatrix} \cos[2\theta(t)] & 0 & \sin[2\theta(t)] \\ 0 & 1 & 0 \\ -\sin[2\theta(t)] & 0 & \cos[2\theta(t)] \end{pmatrix}, \quad (65)$$

$$\mathcal{R}_\theta \dot{\mathcal{R}}_\theta^{-1} = 2\dot{\theta}(t) \begin{pmatrix} 0 & 0 & 1 \\ 0 & 0 & 0 \\ -1 & 0 & 0 \end{pmatrix}, \quad (66)$$

$$\dot{\theta}(t) = \frac{\dot{\Omega}_e(t)\delta(t) - \Omega_e(t)\dot{\delta}(t)}{2(\delta^2(t) + \Omega_e^2(t))}. \quad (67)$$

Neglecting nonadiabatic coupling term  $\mathcal{R}_\theta \dot{\mathcal{R}}_\theta^{-1}$  in equation 63, we obtain

$$\dot{\bar{\mathbf{B}}} = \bar{\mathbf{\Omega}} \times \bar{\mathbf{B}}, \quad (68)$$

where  $\bar{\mathbf{\Omega}} = (0, 0, \lambda(t))$ .

Note that equation 63 can be obtained in a different way starting from equation 31, constructing

equation for the density matrix, and using  $Tr[\sigma_i \rho]$ .

---

## 7. Evolution Operator of the Bloch Vector

---

Since we already know the exact form of the evolution operator  $\mathbf{U}(t)$  in equation 34 and

$$|\Psi(t)\rangle = \mathbf{U}(t)|\Psi(0)\rangle, \quad (69)$$

we can easily construct the evolution operator for the Bloch vector. Using the definition of the density matrix, we have

$$\boldsymbol{\rho}(t) = |\Psi(t)\rangle\langle\Psi(t)| = \mathbf{U}(t)|\Psi(0)\rangle\langle\Psi(0)|\mathbf{U}^\dagger(t) = \mathbf{U}(t)\boldsymbol{\rho}(0)\mathbf{U}^\dagger(t), \quad (70)$$

where

$$\boldsymbol{\rho}(0) = |\Psi(0)\rangle\langle\Psi(0)| = \begin{pmatrix} \varrho_{00}(0) & \varrho_{01}(0) \\ \varrho_{10}(0) & \varrho_{11}(0) \end{pmatrix} = \frac{1}{2} \begin{pmatrix} 1 + w_0 & u_0 - iv_0 \\ u_0 + iv_0 & 1 - w_0 \end{pmatrix}. \quad (71)$$

is the initial condition and

$$\begin{aligned} \mathbf{U}^\dagger(t) &= \begin{pmatrix} \cos(S(t)/2) & -ie^{i\Delta\phi}\sin(S(t)/2) \\ -ie^{-i\Delta\phi}\sin(S(t)/2) & \cos(S(t)/2) \end{pmatrix} \\ &= \cos(S(t)/2)\mathbf{I} - i\sin(S(t)/2)(e^{i\Delta\phi}\boldsymbol{\sigma}_+ + e^{-i\Delta\phi}\boldsymbol{\sigma}_-) \\ &= \cos(S(t)/2)\mathbf{I} + i\sin(S(t)/2)(\mathbf{n} \cdot \boldsymbol{\sigma}) = e^{iS(t)\mathbf{n}\cdot\boldsymbol{\sigma}/2}. \end{aligned} \quad (72)$$

Therefore,

$$\begin{aligned} \boldsymbol{\rho}(t) &= \mathbf{U}(t)\boldsymbol{\rho}(0)\mathbf{U}^\dagger(t) = \begin{pmatrix} \cos(S(t)/2) & ie^{i\Delta\phi}\sin(S(t)/2) \\ ie^{-i\Delta\phi}\sin(S(t)/2) & \cos(S(t)/2) \end{pmatrix} \\ &\begin{pmatrix} \varrho_{00}(0) & \varrho_{01}(0) \\ \varrho_{10}(0) & \varrho_{11}(0) \end{pmatrix} \begin{pmatrix} \cos(S(t)/2) & -ie^{i\Delta\phi}\sin(S(t)/2) \\ -ie^{-i\Delta\phi}\sin(S(t)/2) & \cos(S(t)/2) \end{pmatrix}, \end{aligned} \quad (73)$$

or, exactly,

$$\begin{aligned} \varrho_{00}(t) &= \varrho_{00}(0) \cos^2(S(t)/2) + \varrho_{11}(0) \sin^2(S(t)/2) \\ &+ \frac{i}{2} \sin(S(t)) (\varrho_{10}(0)e^{i\Delta\phi} - \varrho_{01}(0)e^{-i\Delta\phi}) , \end{aligned} \quad (74a)$$

$$\begin{aligned} \varrho_{01}(t) &= -\frac{i}{2} e^{i\Delta\phi} \sin(S(t)) (\varrho_{00}(0) - \varrho_{11}(0)) + \varrho_{10}(0)e^{2i\Delta\phi} \sin^2(S(t)/2) \\ &+ \varrho_{01}(0) \cos^2(S(t)/2) , \end{aligned} \quad (74b)$$

$$\begin{aligned} \varrho_{10}(t) &= \frac{i}{2} e^{-i\Delta\phi} \sin(S(t)) (\varrho_{00}(0) - \varrho_{11}(0)) + \varrho_{01}(0)e^{-2i\Delta\phi} \sin^2(S(t)/2) \\ &+ \varrho_{10}(0) \cos^2(S(t)/2) , \end{aligned} \quad (74c)$$

$$\begin{aligned} \varrho_{11}(t) &= \varrho_{00}(0) \sin^2(S(t)/2) + \varrho_{11}(0) \cos^2(S(t)/2) \\ &+ \frac{i}{2} \sin(S(t)) (\varrho_{01}(0)e^{-i\Delta\phi} - \varrho_{10}(0)e^{i\Delta\phi}) . \end{aligned} \quad (74d)$$

Taking into account equation 41, we obtain for the Bloch vector components

$$\begin{aligned} u(t) &= \sin(S(t)) \sin(\Delta\phi) w_0 + (\cos^2(S(t)/2) + \sin^2(S(t)/2) \cos(2\Delta\phi)) u_0 \\ &- \sin^2(S(t)/2) \sin(2\Delta\phi) v_0 , \end{aligned} \quad (75a)$$

$$\begin{aligned} v(t) &= \sin(S(t)) \cos(\Delta\phi) w_0 - \sin^2(S(t)/2) \sin(2\Delta\phi) u_0 \\ &+ (\cos^2(S(t)/2) - \sin^2(S(t)/2) \cos(2\Delta\phi)) v_0 \end{aligned} \quad (75b)$$

$$\begin{aligned} w(t) &= (\cos^2(S(t)/2) - \sin^2(S(t)/2)) w_0 \\ &- \sin(S(t)) (u_0 \sin(\Delta\phi) + v_0 \cos(\Delta\phi)) , \end{aligned} \quad (75c)$$

which can be presented in the matrix form as

$$\mathbf{B}(t) = \begin{pmatrix} \mathcal{C}^2 + \mathcal{S}^2 \cos(2\Delta\phi) & -\mathcal{S}^2 \sin(2\Delta\phi) & 2\mathcal{C} \cdot \mathcal{S} \sin(\Delta\phi) \\ -\mathcal{S}^2 \sin(2\Delta\phi) & \mathcal{C}^2 - \mathcal{S}^2 \cos(2\Delta\phi) & 2\mathcal{C} \cdot \mathcal{S} \cos(\Delta\phi) \\ -2\mathcal{C} \cdot \mathcal{S} \sin(\Delta\phi) & -2\mathcal{C} \cdot \mathcal{S} \cos(\Delta\phi) & \mathcal{C}^2 - \mathcal{S}^2 \end{pmatrix} \mathbf{B}(0), \quad (76)$$

where  $\mathcal{C} = \cos(S(t)/2)$ ,  $\mathcal{S} = \sin(S(t)/2)$ .

---

## 8. Ultrafast Qubit Rotations Using Geometrical Phase

---

At this point, we are ready to discuss implementation of the single qubit gates since we have obtained the analytic solution for the qubit wave function and constructed the evolution operator in the Bloch vector representation. A universal set of quantum gates has been intensively discussed in the literature related to the universality in quantum computation (9–12). To perform quantum computation, we must have two major building blocks at our disposal: arbitrary unitary operations on a single qubit and a controlled-NOT operation on two qubits. Here we address only single qubit manipulation.

To demonstrate arbitrary geometric operations on a single qubit, we use the Bloch vector representation discussed in the previous section. Since any unitary rotation of the Bloch vector can be decomposed as (9, 13)

$$U = e^{i\alpha_0} \mathbf{R}_z(\alpha_1) \mathbf{R}_y(\alpha_2) \mathbf{R}_z(\alpha_3), \quad (77)$$

where  $\mathbf{R}_i = e^{i\alpha\sigma_i}$  ( $i = y, z$ ) are the rotation operators, we need to demonstrate rotations of the qubit Bloch vector about the  $z$  and  $y$  axes by applying various sequences of external pulses. The decomposition in equation 77 plays an important role in circuit-based quantum computing, as it shows explicitly that two single-qubit operations allow us to create the arbitrary state of the qubit. Here we show how this can be accomplished by controlling the parameters of the external pulses, which are defined by the explicit form of the evolution operator (see equation 34). There are two distinct ways of the implementation depending on which part of the total qubit phase we employ: dynamical or geometrical (14). Quantum gates relying on geometrical quantum phases are called holonomic gates and they are expected to be robust with respect to noise (15, 18, 19).

To implement the rotation of the Bloch vector about  $z$  axis (the phase gate) based on the geometrical phase, we can use the evolution operator of the resonant qubit, equation 34. The product of two evolution operators corresponding to the sequence of two  $\pi$  pulses with the relative phase  $\Delta\phi = \varphi + \pi$ , gives

$$\mathbf{R}_z(\varphi) = U_{\pi;\varphi+\pi} U_{\pi;0} = \begin{pmatrix} e^{i\varphi} & 0 \\ 0 & e^{-i\varphi} \end{pmatrix}, \quad (78)$$

where the first subindex of  $U$  indicates the pulse area,  $S(T)$ , and the second one indicates the phase,  $\Delta\phi$ .

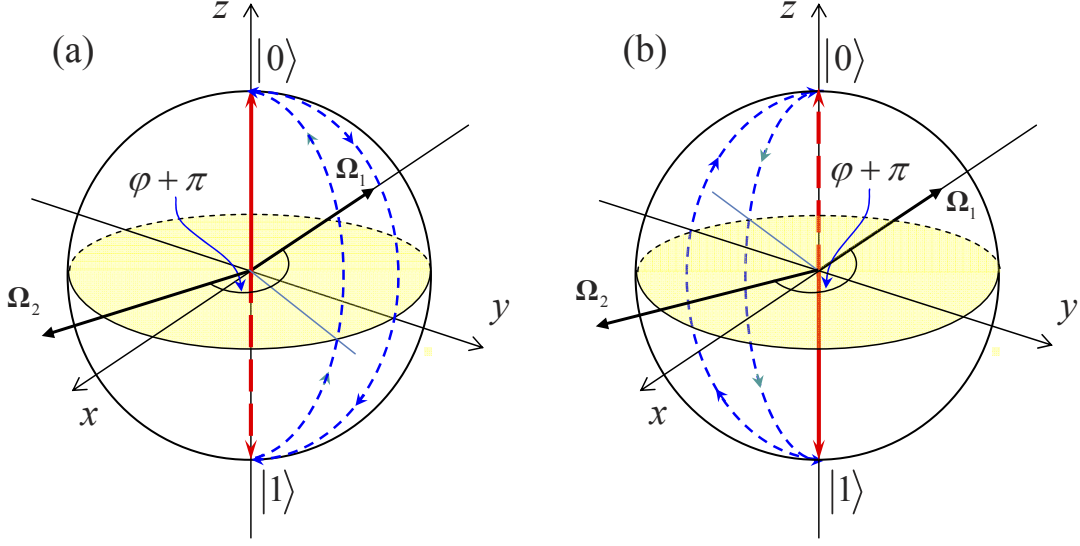


Figure 5. The Bloch vector trajectory for the qubit state  $|0\rangle$  in panel (a) and the qubit state  $|1\rangle$  in panel (b) generated by the sequence of two  $\pi$ -pulses with the relative phase  $\varphi + \pi$ .

Figure 5 shows the Bloch vector trajectories of the qubit basis states  $|0\rangle$  and  $|1\rangle$ , which correspond to the angles  $\beta = 0$  and  $\beta = \pi$  in equation 41 and the Bloch vector initially pointing in  $z$  and  $-z$  directions while the vector  $\Omega_1 = (-\Omega_e, 0, 0)$  is pointing in  $-x$  direction. For simplicity we chose  $\Delta\phi = 0$  for the first  $\pi$ -pulse. The first  $\pi$ -pulse flips the population to the state  $|1\rangle$  ( $|0\rangle$ ); correspondingly, the Bloch vector turns about the effective field vector  $\Omega_1$  (about the  $x$  axis), and it stays in the  $y, z$  plane all the time and points in the  $-z$  ( $z$ ) direction at the end of the pulse. Due to the second  $\pi$ -pulse, the population is transferred back to the initial state  $|0\rangle$  ( $|1\rangle$ ); therefore, the Bloch vector returns to its original position pointing along the  $z$  ( $-z$ ) axis. However, since we chose  $\Delta\phi = \varphi + \pi$  for the second  $\pi$ -pulse, the pseudo-field vector is rotated counterclockwise by the angle  $\varphi + \pi$  in the  $x, y$  plane,  $\Omega_2 = (\Omega_e \cos \varphi, -\Omega_e \sin \varphi, 0)$ , and the Bloch vector moves in the plane perpendicular to the  $x, y$  plane and has the angle  $\pi/2 - \alpha$  ( $-\pi/2 - \alpha$ ) with the  $x, z$  plane.

The Bloch vectors representing a pair of orthogonal basis states  $|0\rangle$  and  $|1\rangle$  follow a path enclosing correspondingly solid angles of  $2\varphi$  and  $-2\varphi$ . The geometrical phase is equal to one half of the solid angle, which means the basis states  $|0\rangle$  and  $|1\rangle$  gain phases  $\varphi$  and  $-\varphi$  and the evolution operator takes the form of the phase gate, equation 78, with the relative phase controlling the phase of the gate.

The rotation operator about the  $y$  axis can be constructed using three pulses. The first and third

pulse is  $\pi/2$ -pulse with  $\Delta\phi = 0$ , while the second pulse is  $\pi$ -pulse with the relative phase  $\pi + \varphi$ . It is easy to show, using equation 34, that this three-pulse sequence results in

$$\mathbf{R}_y(\varphi) = U_{\frac{\pi}{2};0} U_{\pi;\pi+\varphi} U_{\frac{\pi}{2};0} = e^{i\varphi\sigma_y}. \quad (79)$$

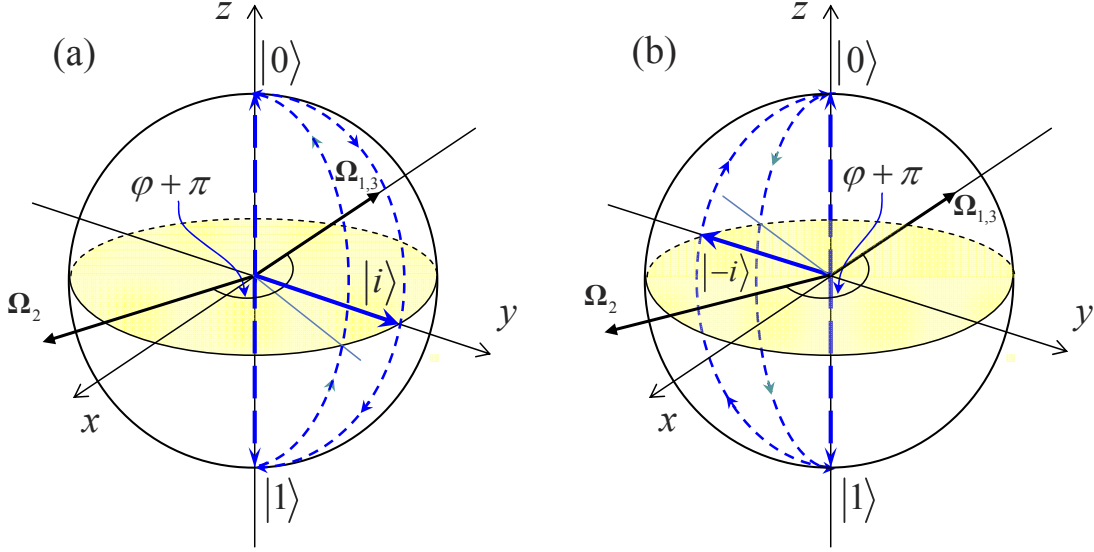


Figure 6. The Bloch vector trajectory for the qubit state  $|i\rangle$  in panel (a) and the qubit state  $|-i\rangle$  in panel (b) generated by the sequence of two  $\pi/2$ -pulses and one  $\pi$  pulse with the relative phase  $\varphi + \pi$ .

To demonstrate the geometrical nature of the  $\mathbf{R}_y(\varphi)$  operation, we use the fact that it creates the relative phase between the qubit basis states  $|\pm i\rangle = (|0\rangle \pm i|1\rangle)/\sqrt{2}$  (see Appendix for the eigenvectors of the Pauli matrices). In the Bloch representation, these states have the form

$$|\pm i\rangle = \cos\left(\frac{\pi}{4}\right)|0\rangle + e^{\pm i\frac{\pi}{2}} \sin\left(\frac{\pi}{4}\right)|1\rangle, \quad (80)$$

which are two vectors defined by the angles  $\beta = \pi/2$  and  $\alpha = \pm\pi/2$  and pointing in the  $y$  and  $-y$  directions, as shown in figure 6. The trajectory of the Bloch vector representing the states  $|\pm i\rangle$  is shown in figure 6. The pseudo-field vectors  $\Omega_1$  and  $\Omega_3$  are defined by the effective Rabi frequencies of the first and third pulses and are pointing in the  $-x$  direction since  $\Delta\phi = 0$ . The second pseudo-field vector  $\Omega_2$  is rotated counterclockwise by the angle  $\varphi + \pi$  in the  $x, y$  plane same as in the case above. The initial Bloch vector is pointing in the  $y$  ( $-y$ ) direction. The first  $\pi/2$ -pulse rotates the Bloch vector about  $\Omega_1$  to the position of the state  $|1\rangle$  ( $|0\rangle$ ). The second pulse flips the direction of the Bloch vector. The third  $\pi/2$ -pulse returns the Bloch vector to its original position. The Bloch vector and the pseudo-field vector are orthogonal during the whole

evolution. Similar to the previous case, we observe that the basis states  $|i\rangle$  and  $|-i\rangle$  follow a path enclosing correspondingly solid angles of  $2\varphi$  and  $-2\varphi$ . Therefore, they gain the relative phase  $2\varphi$ , which is the geometrical phase defined by the relative phase between pulses. It is easy to show that the phase gate in the  $|\pm i\rangle$  basis is equivalent to the  $\mathbf{R}_y(\varphi)$  gate in the  $|0\rangle, |1\rangle$  basis.

---

## 9. Rotation in the Bloch Representation

---

Rotation operations in the Schrödinger picture are

$$|\Psi\rangle = \mathbf{R}_i|\Psi_0\rangle, \quad (81)$$

where  $i = \{x, y, z\}$ ,  $|\Psi_0\rangle$  is the initial wave function,

$$\mathbf{R}_x = e^{i\varphi\sigma_x} = \begin{pmatrix} \cos \varphi & i \sin \varphi \\ i \sin \varphi & \cos \varphi \end{pmatrix}, \quad (82)$$

$$\mathbf{R}_x^{-1} = e^{-i\varphi\sigma_x} = \begin{pmatrix} \cos \varphi & -i \sin \varphi \\ -i \sin \varphi & \cos \varphi \end{pmatrix}, \quad (83)$$

$$\mathbf{R}_y = e^{i\varphi\sigma_y} = \begin{pmatrix} \cos \varphi & \sin \varphi \\ -\sin \varphi & \cos \varphi \end{pmatrix}, \quad (84)$$

$$\mathbf{R}_y^{-1} = e^{-i\varphi\sigma_y} = \begin{pmatrix} \cos \varphi & -\sin \varphi \\ \sin \varphi & \cos \varphi \end{pmatrix}, \quad (85)$$

$$\mathbf{R}_z = e^{i\varphi\sigma_z} = \begin{pmatrix} e^{i\varphi} & 0 \\ 0 & e^{-i\varphi} \end{pmatrix}, \quad (86)$$

$$\mathbf{R}_z^{-1} = e^{-i\varphi\sigma_z} = \begin{pmatrix} e^{-i\varphi} & 0 \\ 0 & e^{i\varphi} \end{pmatrix}. \quad (87)$$

Therefore for the density matrix, we have

$$\boldsymbol{\rho} = |\Psi\rangle\langle\Psi| = \mathbf{R}_i|\Psi_0\rangle\langle\Psi_0|\mathbf{R}_i^{-1} = \mathbf{R}_i\boldsymbol{\rho}_0\mathbf{R}_i^{-1}, \quad (88)$$

where  $\boldsymbol{\rho}_0 = |\Psi_0\rangle\langle\Psi_0|$  is the initial density matrix.

Using equation

$$\mathbf{B} = Tr[\vec{\sigma}\boldsymbol{\rho}] = (Tr[\sigma_x\boldsymbol{\rho}], Tr[\sigma_y\boldsymbol{\rho}], Tr[\sigma_z\boldsymbol{\rho}]) = (u, v, w), \quad (89)$$

we find the following expressions for the transformation of the Bloch vector components

$$u = Tr[\sigma_x\mathbf{R}_i\boldsymbol{\rho}_0\mathbf{R}_i^{-1}], \quad (90)$$

$$v = Tr[\sigma_y\mathbf{R}_i\boldsymbol{\rho}_0\mathbf{R}_i^{-1}], \quad (91)$$

$$w = Tr[\sigma_z\mathbf{R}_i\boldsymbol{\rho}_0\mathbf{R}_i^{-1}]. \quad (92)$$

Substituting equations 82 - 87 into equations 90 - 92, we obtain

$$\mathcal{R}_x = \begin{pmatrix} 1 & 0 & 0 \\ 0 & \cos(2\varphi) & \sin(2\varphi) \\ 0 & -\sin(2\varphi) & \cos(2\varphi) \end{pmatrix}, \quad (93)$$

$$\mathcal{R}_y = \begin{pmatrix} \cos(2\varphi) & 0 & -\sin(2\varphi) \\ 0 & 1 & 0 \\ \sin(2\varphi) & 0 & \cos(2\varphi) \end{pmatrix}, \quad (94)$$

$$\mathcal{R}_z = \begin{pmatrix} \cos(2\varphi) & \sin(2\varphi) & 0 \\ -\sin(2\varphi) & \cos(2\varphi) & 0 \\ 0 & 0 & 1 \end{pmatrix}. \quad (95)$$

From equation 76, we see that the evolution operator in the Bloch representation is

$$\mathcal{U}(t) = \begin{pmatrix} \mathcal{C}^2 + \mathcal{S}^2 \cos(2\Delta\phi) & -\mathcal{S}^2 \sin(2\Delta\phi) & 2\mathcal{C} \cdot \mathcal{S} \sin(\Delta\phi) \\ -\mathcal{S}^2 \sin(2\Delta\phi) & \mathcal{C}^2 - \mathcal{S}^2 \cos(2\Delta\phi) & 2\mathcal{C} \cdot \mathcal{S} \cos(\Delta\phi) \\ -2\mathcal{C} \cdot \mathcal{S} \sin(\Delta\phi) & -2\mathcal{C} \cdot \mathcal{S} \cos(\Delta\phi) & \mathcal{C}^2 - \mathcal{S}^2 \end{pmatrix}. \quad (96)$$

Therefore, to demonstrate, for example, the  $R_z$  rotation in the Bloch picture, we see that the first  $\pi$  pulse with the relative phase  $\Delta\phi = 0$  gives for the evolution operator

$$\mathcal{U}_{\pi;0} = \begin{pmatrix} 1 & 0 & 0 \\ 0 & -1 & 0 \\ 0 & 0 & -1 \end{pmatrix}. \quad (97)$$

The second  $\pi$  pulse with the relative phase  $\Delta\phi = \pi + \varphi$  gives for the evolution operator

$$\mathcal{U}_{\pi;\pi+\varphi} = \begin{pmatrix} \cos(2(\pi + \varphi)) & -\sin(2(\pi + \varphi)) & 0 \\ -\sin(2(\pi + \varphi)) & -\cos(2(\pi + \varphi)) & 0 \\ 0 & 0 & -1 \end{pmatrix}. \quad (98)$$

Finally, the sequence of  $\mathcal{U}_{\pi;\pi+\varphi}$  and  $\mathcal{U}_{\pi;0}$  results in

$$\begin{aligned} \mathcal{U}_{\pi;\pi+\varphi}\mathcal{U}_{\pi;0} &= \begin{pmatrix} \cos(2(\pi + \varphi)) & -\sin(2(\pi + \varphi)) & 0 \\ -\sin(2(\pi + \varphi)) & -\cos(2(\pi + \varphi)) & 0 \\ 0 & 0 & -1 \end{pmatrix} \begin{pmatrix} 1 & 0 & 0 \\ 0 & -1 & 0 \\ 0 & 0 & -1 \end{pmatrix} \\ &= \begin{pmatrix} \cos(2\varphi) & \sin(2\varphi) & 0 \\ -\sin(2\varphi) & \cos(2\varphi) & 0 \\ 0 & 0 & 1 \end{pmatrix}, \end{aligned} \quad (99)$$

which, of course, coincides with equation 95. Similarly, one could consider the  $R_y$  rotation in the Bloch picture.

---

## 10. Generalization of the Single-Qubit Operation Using Bright-Dark Basis

---

In the previous sections, we have considered several excitation schemes of the three-level system and discussed a possible implementation of single-qubit gates. It was shown that all possible qubit states can be created in a controllable fashion using a couple of completely overlapped laser pulses,  $\Omega_P(t) = \Omega_S(t)$ . In this section, we present a bit more general solution, which allow some additional flexibility in terms of the ratio of the pump and Stokes pulse amplitudes. Again, we address here the coherent Raman excitation in a three-level  $\Lambda$ -type system consisting of the two lowest states of electron spin  $|0\rangle \equiv |-X\rangle$  and  $|0\rangle \equiv |X\rangle$  coupled through an intermediate trion state  $|T\rangle$  (see figure 1) and assume that the trion state is far off-resonance with the external fields. In addition, we restrict our consideration to the non-impulsive regime, and can then put

$\bar{\Omega}_{P+}(t) = \bar{\Omega}_{S+}(t) = 0$  in the equation 6 so that the Hamiltonian takes the form

$$\tilde{H} = U_{RWA}^{-1} H U_{RWA} - i\hbar U_{RWA}^{-1} \dot{U}_{RWA} \quad (100)$$

$$= -\frac{\hbar}{2} \begin{pmatrix} 0 & 0 & \Omega_{P+} \\ 0 & -2\omega_B & \Omega_{S+} \\ \Omega_{P+}^* & \Omega_{S+}^* & -2\omega_T \end{pmatrix} + \hbar \begin{pmatrix} 0 & 0 & 0 \\ 0 & -\Delta\omega & 0 \\ 0 & 0 & -\omega_P \end{pmatrix} \quad (101)$$

$$= -\frac{\hbar}{2} \begin{pmatrix} 0 & 0 & \Omega_{P+} \\ 0 & 2(\Delta\omega - \omega_B) & \Omega_{S+} \\ \Omega_{P+}^* & \Omega_{S+}^* & -2\Delta_P \end{pmatrix}, \quad (102)$$

where  $\Delta_P = \omega_T - \omega_P$ ,  $\Delta\omega = \omega_P - \omega_S$ ,  $\Omega_{P+} = \Omega_{P0}(t)e^{i\phi_P(t)}$ ,  $\Omega_{S+} = \Omega_{S0}(t)e^{i\phi_S(t)}$ , and  $\phi_{P,S}(t) = \phi_{P,S} + \alpha_{P,S}t^2/2$ .

Let us consider the case when  $\Omega_{P0}(t) = \Omega_0(t) \cos \vartheta$  and  $\Omega_{S0}(t) = \Omega_0(t) \sin \vartheta$ ; the same time-dependent envelope for the pump and Stokes Rabi frequencies while the mixing angle  $\vartheta$  controls the ration between the maximum of the Rabi frequencies. In this case, we make transformation to the bright-dark basis ( $|\tilde{\Psi}\rangle = \{a_B(t), a_D(t), \tilde{b}(t)\} = \mathcal{R}_{bd}|\tilde{\Psi}\rangle$ ) using the following matrix

$$\mathcal{R}_{bd} = \begin{pmatrix} e^{-i\phi_P} \cos \vartheta & e^{-i\phi_S} \sin \vartheta & 0 \\ -e^{i\phi_S} \sin \vartheta & e^{i\phi_P} \cos \vartheta & 0 \\ 0 & 0 & 1 \end{pmatrix}. \quad (103)$$

$$\mathcal{R}_{bd}^{-1} = \begin{pmatrix} e^{i\phi_P} \cos \vartheta & -e^{-i\phi_S} \sin \vartheta & 0 \\ e^{i\phi_S} \sin \vartheta & e^{-i\phi_P} \cos \vartheta & 0 \\ 0 & 0 & 1 \end{pmatrix}. \quad (104)$$

In the bright-dark basis, the Hamiltonian takes the form

$$\begin{aligned} \bar{H} &= \mathcal{R}_{bd} \tilde{H} \mathcal{R}_{bd}^{-1} \\ &= \frac{\hbar}{2} \begin{pmatrix} 2\delta\mathcal{S}^2 & 2\delta\mathcal{S}\mathcal{C}e^{-i\phi_+} & -\xi_+(t)\Omega_0(t) \\ 2\delta\mathcal{S}\mathcal{C}e^{i\phi_+} & 2\delta\mathcal{C}^2 & e^{i\phi_+}\xi_-(t)\mathcal{S}\mathcal{C}\Omega_0(t) \\ -\xi_+^*(t)\Omega_0(t) & e^{-i\phi_+}\xi_-^*(t)\mathcal{S}\mathcal{C}\Omega_0(t) & 2\Delta_P \end{pmatrix}, \end{aligned} \quad (105)$$

where  $\mathcal{S} = \sin \vartheta$ ,  $\mathcal{C} = \cos \vartheta$ ,  $\phi_+ = \phi_P + \phi_S$ ,  $\xi_+(t) = e^{i\alpha t^2/2}\mathcal{C}^2 + e^{i\beta t^2/2}\mathcal{S}^2$ ,  $\xi_-(t) = e^{i\alpha t^2/2} - e^{i\beta t^2/2}$ .

In the resonant case,  $\delta = 0$ , we obtain

$$\begin{aligned}\bar{\mathbf{H}} &= \mathcal{R}_{bd} \tilde{\mathbf{H}} \mathcal{R}_{bd}^{-1} \\ &= \frac{\hbar}{2} \begin{pmatrix} 0 & 0 & -\xi_+(t)\Omega_0(t) \\ 0 & 0 & e^{i\phi_+}\xi_-(t)\mathcal{SC}\Omega_0(t) \\ -\xi_+^*(t)\Omega_0(t) & e^{-i\phi_+}\xi_-^*(t)\mathcal{SC}\Omega_0(t) & 2\Delta_P \end{pmatrix}.\end{aligned}\quad (106)$$

In the case of equal chirp rates,  $\alpha = \beta$ , we have

$$\begin{aligned}\bar{\mathbf{H}} &= \mathcal{R}_{bd} \tilde{\mathbf{H}} \mathcal{R}_{bd}^{-1} \\ &= \frac{\hbar}{2} \begin{pmatrix} 2\delta\mathcal{S}^2 & 2\delta\mathcal{SC}e^{-i\phi_+} & -e^{i\alpha t^2/2}\Omega_0(t) \\ 2\delta\mathcal{SC}e^{i\phi_+} & 2\delta\mathcal{C}^2 & 0 \\ -e^{-i\alpha t^2/2}\Omega_0(t) & 0 & 2\Delta_P \end{pmatrix}.\end{aligned}\quad (107)$$

In the two-photon resonance case,  $\delta = 0$ , and equal chirp rates,  $\alpha = \beta$ , we have

$$\begin{aligned}\bar{\mathbf{H}} &= \mathcal{R}_{bd} \tilde{\mathbf{H}} \mathcal{R}_{bd}^{-1} \\ &= \frac{\hbar}{2} \begin{pmatrix} 0 & 0 & -e^{i\alpha t^2/2}\Omega_0(t) \\ 0 & 0 & 0 \\ -e^{-i\alpha t^2/2}\Omega_0(t) & 0 & 2\Delta_P \end{pmatrix}.\end{aligned}\quad (108)$$

We can see from equation 108 that  $a_D(t) = a_D(0)$  and we are left with the system of two differential equations for the probability amplitudes  $a_B(t)$  and  $\tilde{b}(t)$ . Making the adiabatic elimination of the excited state  $|T\rangle$  (assuming that  $\dot{\tilde{b}}(t) \approx 0$ ), we have

$$\tilde{b}(t) = \frac{1}{2\Delta_P} \Omega_0(t) e^{-i\alpha t^2/2} a_B(t),\quad (109)$$

and

$$i\dot{a}_B(t) = -\frac{1}{4\Delta_P} \Omega_0^2(t) a_B(t).\quad (110)$$

The solution of the equation 110 is

$$a_B(t) = a_B(0) e^{\frac{i}{4\Delta_P} \int_0^t \Omega_0^2(t') dt'}.\quad (111)$$

Therefore, the evolution operator for the two-photon resonant excitation by the equally chirped

pulses under condition of the adiabatic elimination of the trion state has the following form

$$\begin{aligned}
\mathbf{U}(t) &= \mathcal{R}_{bd}^{-1} \begin{pmatrix} e^{\frac{i}{4\Delta_P} \int_0^t \Omega_0^2(t') dt'} & 0 & 0 \\ 0 & 1 & 0 \\ 0 & 0 & 1 \end{pmatrix} \mathcal{R}_{bd} \\
&= \begin{pmatrix} e^{i\phi_P} \cos \vartheta & -e^{-i\phi_S} \sin \vartheta & 0 \\ e^{i\phi_S} \sin \vartheta & e^{-i\phi_P} \cos \vartheta & 0 \\ 0 & 0 & 1 \end{pmatrix} \begin{pmatrix} e^{iS(t)} & 0 & 0 \\ 0 & 1 & 0 \\ 0 & 0 & 1 \end{pmatrix} \begin{pmatrix} e^{-i\phi_P} \cos \vartheta & e^{-i\phi_S} \sin \vartheta & 0 \\ -e^{i\phi_S} \sin \vartheta & e^{i\phi_P} \cos \vartheta & 0 \\ 0 & 0 & 1 \end{pmatrix} \\
&= \begin{pmatrix} e^{iS(t)} \cos^2 \vartheta + \sin^2 \vartheta & e^{i\Delta\phi} (e^{iS(t)} - 1) \sin \vartheta \cos \vartheta & 0 \\ e^{-i\Delta\phi} (e^{iS(t)} - 1) \sin \vartheta \cos \vartheta & \cos^2 \vartheta + e^{iS(t)} \sin^2 \vartheta & 0 \\ 0 & 0 & 1 \end{pmatrix}, \tag{112}
\end{aligned}$$

where  $S(t) = \int_0^t \Omega_0^2(t') dt' / (4\Delta_P)$ , and  $\Delta\phi = \phi_P - \phi_S$ .

For the qubit states, the evolution operator can be written as

$$\begin{aligned}
\mathbf{U}(t) &= e^{iS(t)/2} \begin{pmatrix} e^{iS(t)/2} \cos^2 \vartheta + e^{-iS(t)/2} \sin^2 \vartheta & e^{i\Delta\phi} (e^{iS(t)/2} - e^{-iS(t)/2}) \sin \vartheta \cos \vartheta \\ e^{-i\Delta\phi} (e^{iS(t)/2} - e^{-iS(t)/2}) \sin \vartheta \cos \vartheta & e^{-iS(t)/2} \cos^2 \vartheta + e^{iS(t)/2} \sin^2 \vartheta \end{pmatrix} \\
&= e^{iS(t)/2} \begin{pmatrix} \cos(S(t)/2) + i \sin(S(t)/2) \cos(2\vartheta) & ie^{i\Delta\phi} \sin(S(t)/2) \sin(2\vartheta) \\ ie^{-i\Delta\phi} \sin(S(t)/2) \sin(2\vartheta) & \cos(S(t)/2) - i \sin(S(t)/2) \cos(2\vartheta) \end{pmatrix} \\
&= e^{iS(t)/2} [\cos(S(t)/2) \mathbf{I} + i \sin(S(t)/2) (\cos(\Delta\phi) \sin(2\vartheta) \boldsymbol{\sigma}_x \\
&\quad - \sin(\Delta\phi) \sin(2\vartheta) \boldsymbol{\sigma}_y + \cos(2\vartheta) \boldsymbol{\sigma}_z)] \\
&= e^{iS(t)/2} e^{-iS(t)\mathbf{n}\cdot\boldsymbol{\sigma}/2}, \tag{113}
\end{aligned}$$

where

$$\mathbf{n} = (-\cos(\Delta\phi) \sin(2\vartheta), \sin(\Delta\phi) \sin(2\vartheta), -\cos(2\vartheta)). \tag{114}$$

---

## 11. Electron Spin in a Quantum Dot as a Qubit

---

In the previous sections, we developed several methods of an arbitrary manipulation of a qubit wave function using the geometric phase. Now we apply the proposed scheme to electron spin states in a charged quantum dot. Due to quantum confinement, the state of the electron can be expressed as a product of the Bloch function and an envelope function, which has a typical scale of the quantum dot size, a few nanometers. The energy level structure and optical selection rules

have been discussed in the literature (1–4). A commonly accepted energy level structure is comprised of four levels, the two electron spin states and two trion spin states. Figure 7 shows two arrangements of the energy levels and polarization selection rules, which provide a possibility of optical control for the electron spin qubit.

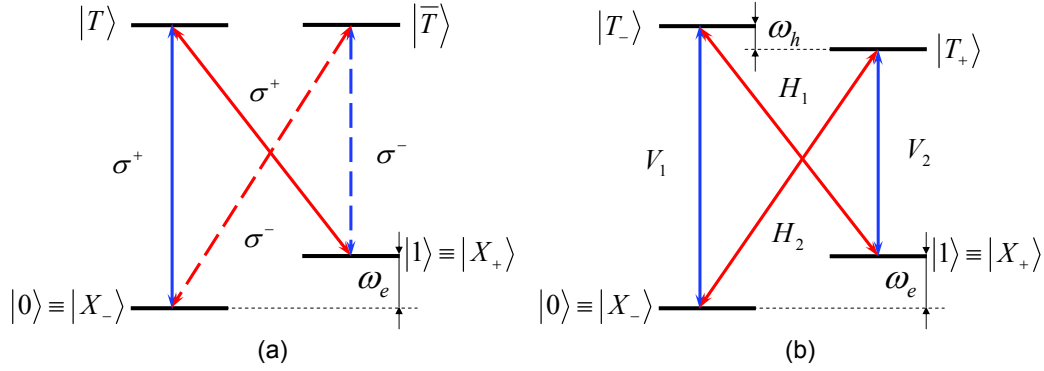


Figure 7. Optical selection rules in different bases.

The usual experiment of the electron spin control is performed at low temperature ( $\sim 1$  K). An external magnetic field in the Voigt configuration (of order  $2 \div 7$  T) is applied along the  $x$ -axis, perpendicular to the sample growth direction, the  $z$  axis. Zeeman splitting of the electron and trion spin states are on the order  $\omega_e = 10$  meV and  $\omega_h = 10\mu\text{eV}$ , correspondingly. At these conditions, taking into account the optical selection rules, the four-level system can be considered as a double  $\Lambda$  system (1–4, 25). This coupling scheme is shown in figure 7(b), where we indicated by “ $H$ ” and “ $V$ ” the optical field couplings with the orthogonal polarization. The shown coupling scheme is in the so-called “ $x$  basis.”

An alternative arrangement is depicted in figure 7(a). In this case the mixed basis is used, where the electron spin states are in the  $x$  basis while the trion states are in the  $z$  basis (1–4, 25). Using the two  $\sigma^+$  or  $\sigma^-$  polarized fields, one can couple the electron spin states  $|X_- \rangle$  and  $|X_+ \rangle$  as shown in the figure 7(a). This is the case where our three-level model can be implemented. The corresponding Hamiltonian has the form obtained in equation 16. Assuming large detunings of the pump and Stokes field frequencies from the transition frequencies to the trion state  $|T \rangle$ , after the adiabatic elimination of the trion state, for the case of completely overlapped, identically linearly chirped pump and Stokes pulses, we obtain the following Hamiltonian

$$\mathbf{H} = -\frac{\hbar}{2} \begin{pmatrix} \delta & \Omega_e(t)e^{i\Delta\phi} \\ \Omega_e^*(t)e^{-i\Delta\phi} & -\delta \end{pmatrix}, \quad (115)$$

where  $\delta = \omega_e - \Delta\omega$ , and  $\Delta\omega = \omega_P - \omega_S$ ,  $\Omega_e(t) = \Omega_{P0}(t)\Omega_{S0}(t)[1 + e^{-i(\Delta\phi + \Delta\omega t)}]^2/(2\Delta)$  is the effective two-photon Rabi frequency,  $\Delta = \omega_T - \omega_P$ , and  $\Delta\phi = \phi_P - \phi_S$ . Note, that here we have used  $\mu_{0T} \approx \mu_{1T}$ .

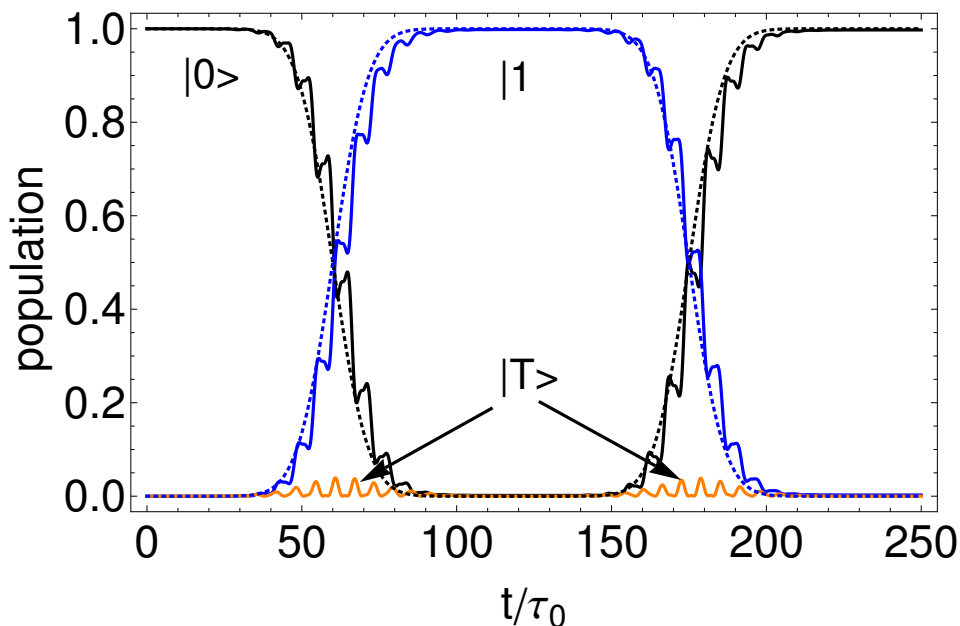


Figure 8. The population dynamics of the resonant qubit states with (dotted lines) and without (solid lines) adiabatic elimination of the trion state in the three-level system. The excitation is generated by the sequence of two pairs of  $\pi$ -pulses (Gaussian pulse envelopes) with the relative phase  $\Delta\varphi = \pi/2$ .

We observe almost perfect resemblance between equation 115 and equation 25. The only difference is that the effective two-photon Rabi frequency contains the oscillating term with a frequency  $\Delta\omega$ . Now, we show that the contribution of this oscillating term can be neglected when the pulse duration is longer than  $\Delta\omega^{-1} \approx \omega_e^{-1}$ . To demonstrate this and justify the procedure of the adiabatic elimination of the trion state, we numerically solve the time-dependent Schrödinger equation with the Hamiltonian in equation 16. That is, we compare our analytic solution with the exact solution of the Schrödinger equation without the adiabatic elimination approximation. An example of the comparison is shown in figure 8.

The example in figure 8 shows the dynamics of the population of the resonant qubit excited by a sequence of two pairs of linearly chirped pulses with the relative phase between the pairs being  $\phi = \pi/2$ . The parameters of the excitations are the transform-limited pulse duration  $\tau_0 = 100$  fs, the pulse area of the pump and Stokes pulses is equal to  $\pi$ , linear chirp rate  $\alpha'/\tau_0^2 = 20$ ,  $\Delta\tau_0 = 6$ ,  $\omega_e\tau_0 = 1$ , the ratio between the maximum Rabi frequency and the single-photon detuning

$\Omega_0/\Delta = 0.77$ . We observe a negligibly small amount of population in the trion state  $|T\rangle$  at the intermediate time. The presented comparison also demonstrates a reasonable agreement between the proposed control schemes and the exact numerical solution. Note that the total time for the qubit operation in figure 8 is on the order of 25 ps, which is much shorter than the typical life time of the trion state (1, 2, 25) as well as the time scale of other forms of decoherence, such as that induced by the electron-phonon interaction.

---

## 12. Conclusion

---

We presented the analytic expression of the evolution operator of the electron spin in a quantum dot, which provides a clear geometrical interpretation of qubit dynamics. Using the analytic form of the evolution operator, we proposed a set of single-qubit rotations that are solely based on the geometrical phase. Our proposal combines the pulse area control with the adiabaticity by using chirped pulses. To estimate the time scale of the proposed operation, we can use the 100 fs pulses, which become picosecond pulses after linearly chirping. That amount of chirping is sufficient to provide adiabatic excitation (6, 7, 20) and can be readily produced experimentally using commercially available laser systems. Using parameters of the dipole moments  $\mu_{0T,T1} \approx 200$  D available in InGaN/GaN (21), GaN/AlN (22, 23) quantum dots, and detuning  $\Delta = 5$  meV, we estimate the peak amplitude of the pulses on the order of  $10^6 - 10^7$  V/m. Note that the demonstrated adiabatic manipulation of a qubit using only the geometric phase has some advantages, since it reduces the requirements of perfect tuning of the control field parameters and is significantly more robust against noise (15, 18, 19).

---

## 13. References

---

1. Press D.; Ladd T. D.; Zhang B.; Yamamoto Y. *Nature* **2008**, *456*, 218–221.
2. Liu R.-B.; Yao W.; Sham L. J. *Adv. Phys.* **2010**, *59*, 703–802.
3. Chen P.; Piermarocchi C.; Sham L. J.; Gammon D.; Steel D. G. *Phys. Rev. A* **2004**, *69*, 075320.
4. Economou S. E.; Reinecke T. L. *Phys. Rev. Lett.* **2007**, *99*, 217401.
5. Bayer M.; Ortner G.; Stern O.; Kuther A.; Gorbunov A. A.; Forchel A.; Hawrylak P.; Fafard S.; Hinzer K.; Reinecke T. L.; Walck S. N.; Reithmaier J. P.; Klopff F.; Schäfer F. *Phys. Rev. B* **2002**, *65*, 195315.
6. Malinovsky V. S.; Krause J. L. *Phys. Rev. A* **2001**, *63*, 043415.
7. Malinovsky V. S.; Krause J. L. *Eur. Phys. J. D* **2001**, *14*, 147–155.
8. Berman P. R.; Malinovsky V. S. *Principles of Laser Spectroscopy and Quantum Optics*; Princeton University Press: Princeton, NJ, 2011.
9. Nielsen M. A.; Chuang I. L. *Quantum Computation and Quantum Information*; Cambridge University Press, 2006.
10. Lloyd S. *Phys. Rev. Lett.* **1995**, *75*, 346–349.
11. Deutsch D.; Barenco A.; Ekert A. *Proc. R. Soc. London Ser. A* **1995**, *449*, 669–677.
12. DiVincenzo D. P.; *Fortschr. Phys.* **2000**, *48*, 771–783.
13. Nakahara M.; Ohmi T. *Quantum computing*; CRC Press: Boca Raton, 2008.
14. Bohm A.; Mostafazadeh A.; Koizumi H.; Niu Q.; Zwanziger J. *The Geometrical Phase in Quantum Systems*; Springer: Berlin, 2003.
15. Zanardi P.; Rasetti M. *Phys. Lett. A* **1999**, *264*, 94–99.
16. Jones, J. A.; Vedral, V.; Ekert, A.; Castagnoli, G.; *Nature* **2000**, *403*, 869–871.
17. Falci, G.; Fazio, R.; Palma, G. M.; Siewert, J.; Vedral, V.; *Nature* **2000**, *407*, 355–358.

18. De Chiara G.; Palma G. M. *Phys. Rev. Lett.* **2003**, *91*, 090404.
19. Lupo C.; Aniello P. *Phys. Scr.* **2009**, *79*, 065012.
20. Malinovskaya S. A.; Malinovsky V. S. *Opt. Lett.* **2007**, *32*, 707–709.
21. Ostapenko I. A.; Höning G.; Kindel C.; Rodt S.; Strittmatter A. *Appl. Phys. Lett.* **2010**, *97*, 063103.
22. Andreev A. D.; O'Reilly E. P. *Appl. Phys. Lett.* **2001**, *79*, 521-523.
23. Ranjan V.; Allan G.; Priester C.; Delerue C. *Phys. Rev. B* **2003**, *68*, 115305.
24. Merzbacher E. *Quantum mechanics*; Wiley: New York, 1998.
25. Greilich, A.; Yakovlev, D. R.; Shabaev, A.; Efros, Al. L.; Yugova, I. A.; Oulton, R.; Stavarache, V.; Wieck, A.; Bayer, M.; *Science* **2006**, *313*, 341–345.

INTENTIONALLY LEFT BLANK.

---

## Appendix. Eigenvectors of the Pauli matrices

---

The eigenstates of  $\sigma_x$  are

$$|j\rangle = \frac{(|0\rangle + |1\rangle)}{\sqrt{2}} = \cos\left(\frac{\pi}{4}\right) |0\rangle + \sin\left(\frac{\pi}{4}\right) |1\rangle = \frac{1}{\sqrt{2}} \begin{pmatrix} 1 \\ 1 \end{pmatrix}, \quad (\text{A-1})$$

$$|-j\rangle = \frac{(|0\rangle - |1\rangle)}{\sqrt{2}} = \cos\left(\frac{\pi}{4}\right) |0\rangle + e^{i\pi} \sin\left(\frac{\pi}{4}\right) |1\rangle = \frac{1}{\sqrt{2}} \begin{pmatrix} 1 \\ -1 \end{pmatrix}. \quad (\text{A-2})$$

Correspondingly,

$$|j\rangle \leftrightarrow \mathbf{B} = \begin{pmatrix} 1 \\ 0 \\ 0 \end{pmatrix} \text{ and } \beta = \frac{\pi}{2}, \alpha = 0, \quad (\text{A-3})$$

$$|-j\rangle \leftrightarrow \mathbf{B} = \begin{pmatrix} -1 \\ 0 \\ 0 \end{pmatrix} \text{ and } \beta = \frac{\pi}{2}, \alpha = \pi. \quad (\text{A-4})$$

The eigenstates of  $\sigma_y$  are

$$|i\rangle = \frac{(|0\rangle + i|1\rangle)}{\sqrt{2}} = \cos\left(\frac{\pi}{4}\right) |0\rangle + e^{i\pi/2} \sin\left(\frac{\pi}{4}\right) |1\rangle = \frac{1}{\sqrt{2}} \begin{pmatrix} 1 \\ i \end{pmatrix}, \quad (\text{A-5})$$

$$|-i\rangle = \frac{(|0\rangle - i|1\rangle)}{\sqrt{2}} = \cos\left(\frac{\pi}{4}\right) |0\rangle + e^{i3\pi/2} \sin\left(\frac{\pi}{4}\right) |1\rangle = \frac{1}{\sqrt{2}} \begin{pmatrix} 1 \\ -i \end{pmatrix}. \quad (\text{A-6})$$

Correspondingly,

$$|i\rangle \leftrightarrow \mathbf{B} = \begin{pmatrix} 0 \\ 1 \\ 0 \end{pmatrix} \text{ and } \beta = \frac{\pi}{2}, \alpha = \frac{\pi}{2}, \quad (\text{A-7})$$

$$|-i\rangle \leftrightarrow \mathbf{B} = \begin{pmatrix} 0 \\ -1 \\ 0 \end{pmatrix} \text{ and } \beta = \frac{\pi}{2}, \alpha = \frac{3\pi}{2}. \quad (\text{A-8})$$

The eigenstates of  $\sigma_z$  are

$$|0\rangle = \begin{pmatrix} 1 \\ 0 \end{pmatrix}, \quad (\text{A-9})$$

$$|1\rangle = \begin{pmatrix} 0 \\ 1 \end{pmatrix}. \quad (\text{A-10})$$

Correspondingly,

$$|0\rangle \leftrightarrow \mathbf{B} = \begin{pmatrix} 0 \\ 0 \\ 1 \end{pmatrix} \text{ and } \beta = 0, \alpha \text{ is arbitrary}, \quad (\text{A-11})$$

$$|1\rangle \leftrightarrow \mathbf{B} = \begin{pmatrix} 0 \\ 0 \\ -1 \end{pmatrix} \text{ and } \beta = \pi, \alpha \text{ is arbitrary}. \quad (\text{A-12})$$

<u>NO. OF COPIES</u>	<u>ORGANIZATION</u>
1 (PDF)	DEFENSE TECHNICAL INFORMATION CTR DTIC OCA
2 (PDF)	DIRECTOR US ARMY RESEARCH LAB RDRL CIO LL IMAL HRA MAIL & RECORDS MGMT
1 (PDF)	GOVT PRINTG OFC A MALHOTRA
2 (PDF)	DIRECTOR US ARMY RESEARCH LAB RDRL SEE M V MALINOVSKY S RUDIN

INTENTIONALLY LEFT BLANK.